AN EXPERIMENTAL DETERMINATION OF THE AERODYNAMIC DRAG CHARACTERISTICS OF VARIABLE GEOMETRY RIGID BODIES

Larry David Pfitzenmaier

NAVAL POSTGRADUATE SCHOOL
Monterey, California

THESIS

An Experimental Determination of the Aerodynamic Drag Characteristics of Variable Geometry Rigid Bodies

by

Larry David Pfitzenmaier

September 1976

Thesis Advisor: D. M. Layton

Approved for public release; distribution unlimited.

SECURITY CLASSIFICATION OF THIS PAGE (When Data Entered)

REPORT DOCUMENTATION PAGE

READ INSTRUCTIONS BEFORE COMPLETING FORM

1. REPORT NUMBER	2. GOVT ACCESSION NO. / 3. RECIPIENT'S CATALOG NUMBER
4. TITLE (and Subtitle): An Experimental Determination of the Aerodynamic Drag Characteristics of Variable Geometry Rigid Bodies	5. TYPE OF REPORT & PERIOD COVERED: Master's Thesis; September 1976
	6. PERFORMING ORG. REPORT NUMBER
7. AUTHOR(s): Larry David Pfitzenmaier	8. CONTRACT OR GRANT NUMBER(s)
9. PERFORMING ORGANIZATION NAME AND ADDRESS: Naval Postgraduate School, Monterey, California 93940	10. PROGRAM ELEMENT, PROJECT, TASK AREA & WORK UNIT NUMBERS
11. CONTROLLING OFFICE NAME AND ADDRESS: Naval Postgraduate School, Monterey, California 93940	12. REPORT DATE: September 1976
	13. NUMBER OF PAGES: 59
14. MONITORING AGENCY NAME & ADDRESS (if different from Controlling Office): Naval Postgraduate School, Monterey, California 93940	15. SECURITY CLASS. (of this report): Unclassified
	15a. DECLASSIFICATION/DOWNGRADING SCHEDULE

16. DISTRIBUTION STATEMENT (of this Report)

Approved for public release; distribution unlimited

17. DISTRIBUTION STATEMENT (of the abstract entered in Block 20, if different from Report)

18. SUPPLEMENTARY NOTES

19. KEY WORDS (Continue on reverse side if necessary and identify by block number)

Variable Geometry Rigid Body
VGRB
Low Speed Wind Tunnel
Coefficient of Drag
Aerodynamic Drag
External Wind Tunnel Balance

20. ABSTRACT (Continue on reverse side if necessary and identify by block number)

An investigation was made of the aerodynamic drag characteristics of two Variable Geometry Rigid Bodies (VGRB's). Results were obtained experimentally through the use of a low speed wind tunnel and an external wind-tunnel balance. Four wood models were tested representing two unique VGRB's in the full-volume and half-volume configurations. Results obtained with the smaller VGRB were compared to those obtained from an elongated

body of revolution of equal length and volume.

An Experimental Determination of the Aerodynamic Drag Characteristics of Variable Geometry Rigid Bodies

by

Larry David Pfitzenmaier
Lieutenant Commander, United States Navy
B.S., Iowa State University, 1967

Submitted in partial fulfillment of the
requirements for the degree of

MASTER OF SCIENCE IN AERONAUTICAL ENGINEERING

from the

NAVAL POSTGRADUATE SCHOOL
September 1976

ABSTRACT

An investigation was made of the aerodynamic drag characteristics of two Variable Geometry Rigid Bodies (VGRB's). Results were obtained experimentally through the use of a low speed wind tunnel and an external wind-tunnel balance. Four wood models were tested representing two unique VGRB's in the full-volume and half-volume configurations. Results obtained with the smaller VGRB were compared to those obtained from an elongated body of revolution of equal length and volume.

TABLE OF CONTENTS

LIST OF FIGURES

LIST OF TABLES

ACKNOWLEDGEMENT

The author is indebted to several people for their assistance in the completion of this investigation. A special debt of gratitude is owed to Associate Professor Donald M. Layton, whose ideas provided the foundation for this project. His unique combination of inspiration, humor, and technical knowledge made this investigation both stimulating and educationally rewarding.

The model fabrication and wind tunnel balance installation were accomplished by Department of Aeronautics technical personnel under the direction of Mr. Robert Besel and Mr. Theodore Dunton. The author is especially grateful to Mr. Robert Ramaker who painstakingly constructed the wind tunnel models and the corresponding model support equipment, and to Mr. Stanley Johnson who provided invaluable assistance in tunnel/balance operation, model installation, and pitch-angle calibration. The photographs contained in this report were taken by the author.

The author also wishes to acknowledge with gratitude the opportunity for postgraduate education provided by the United States Navy.

I. INTRODUCTION

The purpose of this investigation was to determine the aerodynamic drag characteristics of what shall be called a Variable Geometry Rigid Body or VGRB. This was accomplished with the aid of a low speed wind tunnel and an external wind tunnel balance. The results were compared to the experimentally determined aerodynamic drag characteristics of an elongated body of revolution of equal volume.

A VGRB is a device composed of four flat rectangular plates and sixteen flat triangular plates that are connected at their perimeters to form a single, three-dimensional structure whose volume may be varied without destroying structrual integrity. A VGRB in the full-volume configuration appears as a parallelepiped with square cross section and identical pyramid-shaped end sections as shown in Figure 1.

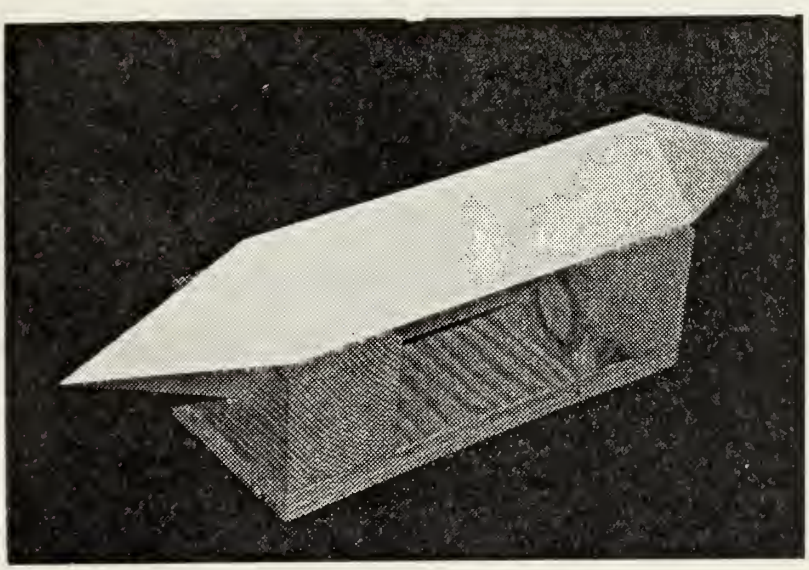

FIGURE 1. FULL-VOLUME VGRB

A VGRB in the zero-volume configuration appears as a flat rectangular plate with identical twin-triangular sections on both ends.

An intermediate-volume VGRB appears as a parallelepiped with rhombic cross section and identical, eight-sided end sections as shown in Figure 2.

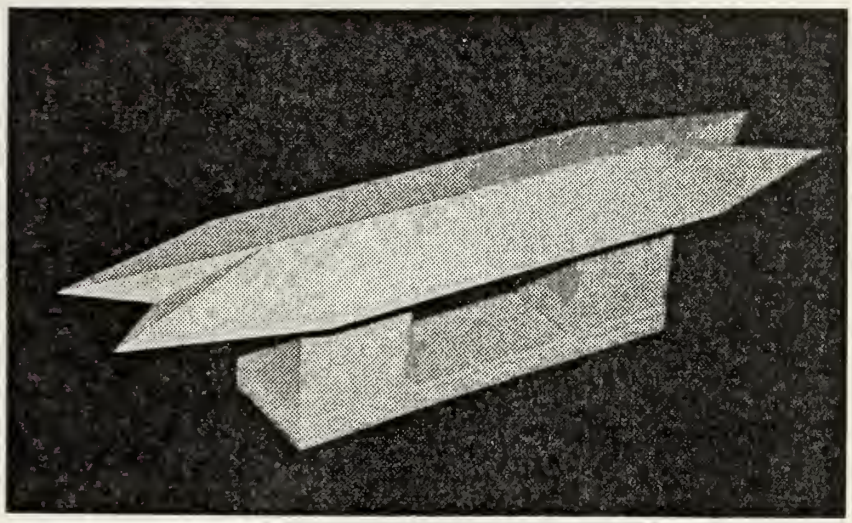

Figure 2. INTERMEDIATE-VOLUME VGRB

It has been suggested that a VGRB may have merit as an externally mounted aircraft fuel tank whose volume, frontal area, and hence aerodynamic drag would be reduced as fuel is consumed. This investigation has shown that as pitch angle is varied such is not necessarily the case.

Two distinct Variable Geometry Rigid Bodies were investigated. Both had the same parallelepiped center section dimensions but varied as to the length of the end sections. Thus the volume of the longer VGRB was slightly greater than that of the shorter one, given the same configuration.

It was decided that the actual construction of hinged, variable-volume VGRB's was not required in order to accomplish the objectives of this investigation. Instead, two solid fir wood models representing the full-volume and half-volume configurations were constructed for each of the VGRB's to be tested. Thus the four models tested correspond to two VGRB's as shown in Figure 3.

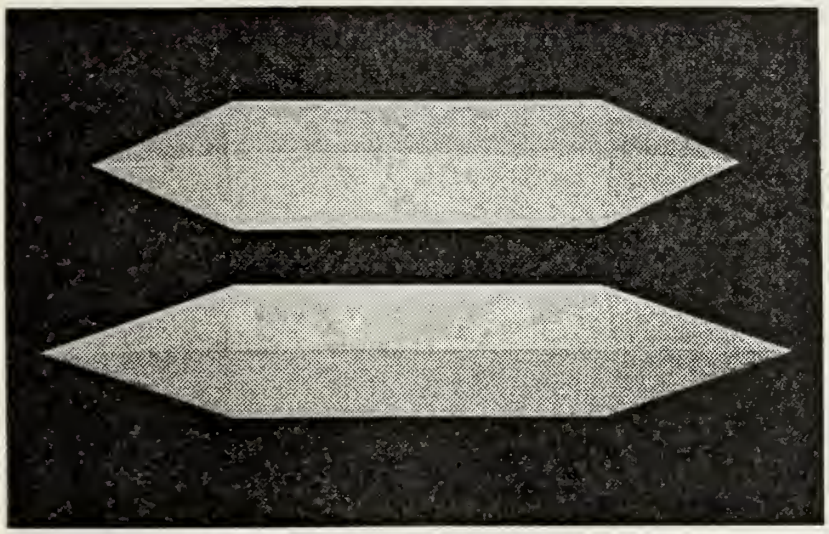

a. Full-Volume

b. Half-Volume

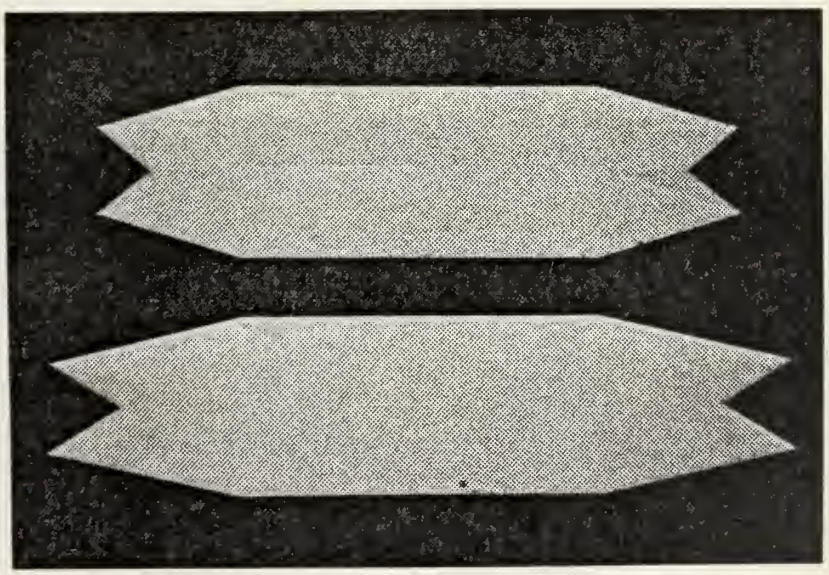

FIGURE 3. SHORT AND LONG VGRB MODELS

A prolate spheroid, generated by revolving an ellipse about its major axis, was constructed so that its volume and length were equal to that of the full-volume model of the short VGRB. The short VGRB and the prolate spheroid are shown in Figure 4. A comparison of the aerodynamic drag due to these two models proved to be of considerable interest.

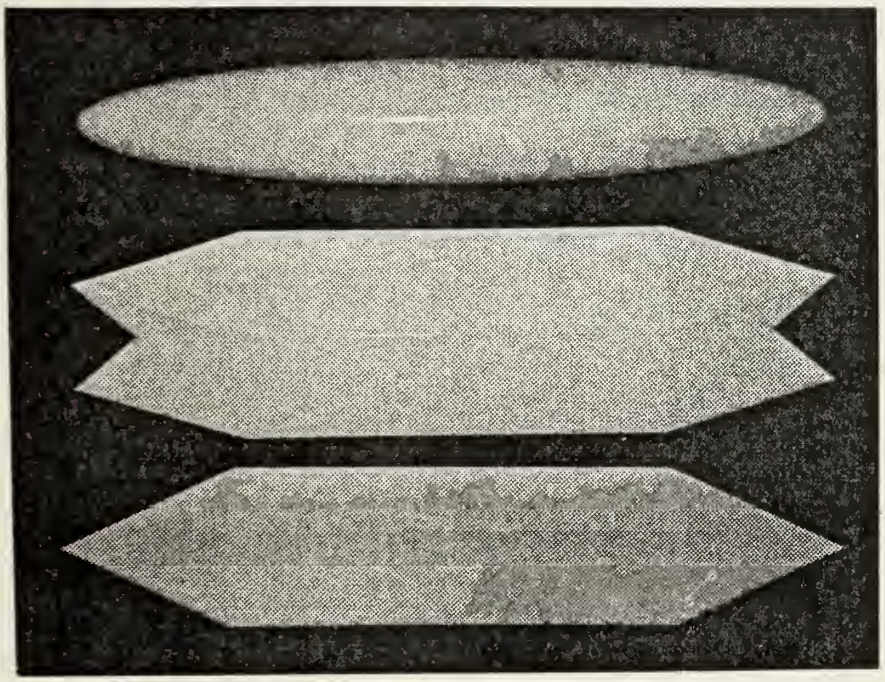

a. Top View

b. Front View

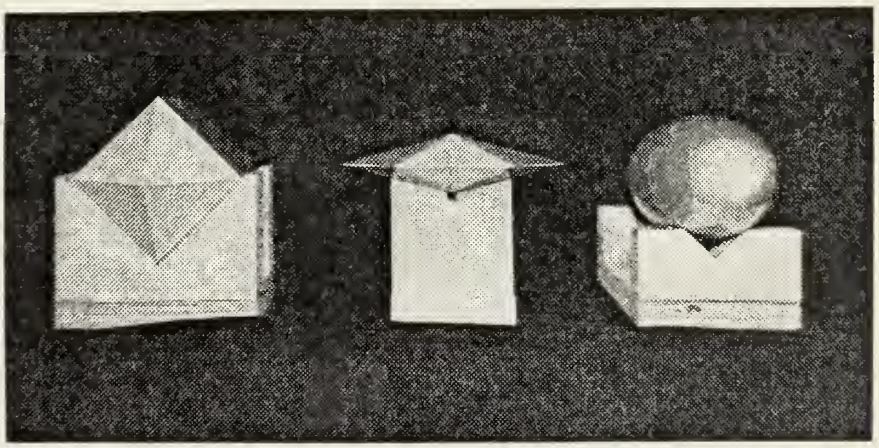

FIGURE 4. SHORT VGRB AND PROLATE SPHEROID

Aerodynamic drag data were obtained at tunnel dynamic pressures of ten and forty-five centimeters of water (approximately ninety and one-hundred-ninety miles per hour). Tabular and graphical representation of results obtained are presented in the appendices of this report.

Model design and construction was accomplished during the third quarter of Fiscal Year 1976 and experimental data were obtained during the fourth quarter of the same year. The facilities of the U. S. Naval Postgraduate School, Monterey, California, were used throughout this investigation.

II. U. S. NAVAL POSTGRADUATE SCHOOL LOW SPEED WIND TUNNEL

The U. S. Naval Postgraduate School low-speed wind tunnel was designed by the Aerolab Development Company of Pasadena, California, and installed in the mid 1950's. A diagram of this tunnel is shown in Figure 6. It is a single-return tunnel measuring sixty-four feet in overall length and approximately twenty-five feet in width.

The power section of the tunnel consists of a one-hundred horsepower electric motor coupled to a three-bladed variable pitch fan by a four-speed truck transmission. Maximum tunnel speed is approximately two-hundred miles per hour.

The test section of the tunnel has a cross-sectional area of 9.88 square feet, approximately one-tenth that of the settling chamber. It is basically rectangular in design but is modified with frosted glass light fillets to provide illumination of the test model. An axial view of the test section is shown in Figure 5.

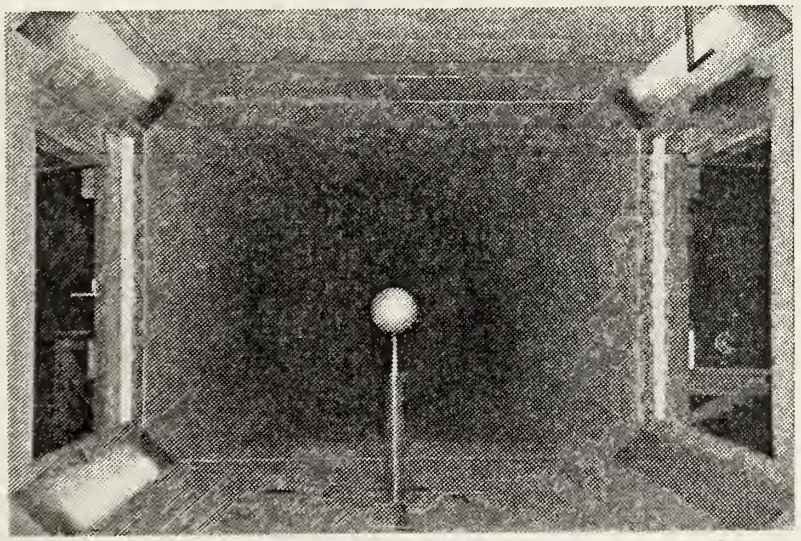

FIGURE 5. WIND TUNNEL TEST SECTION

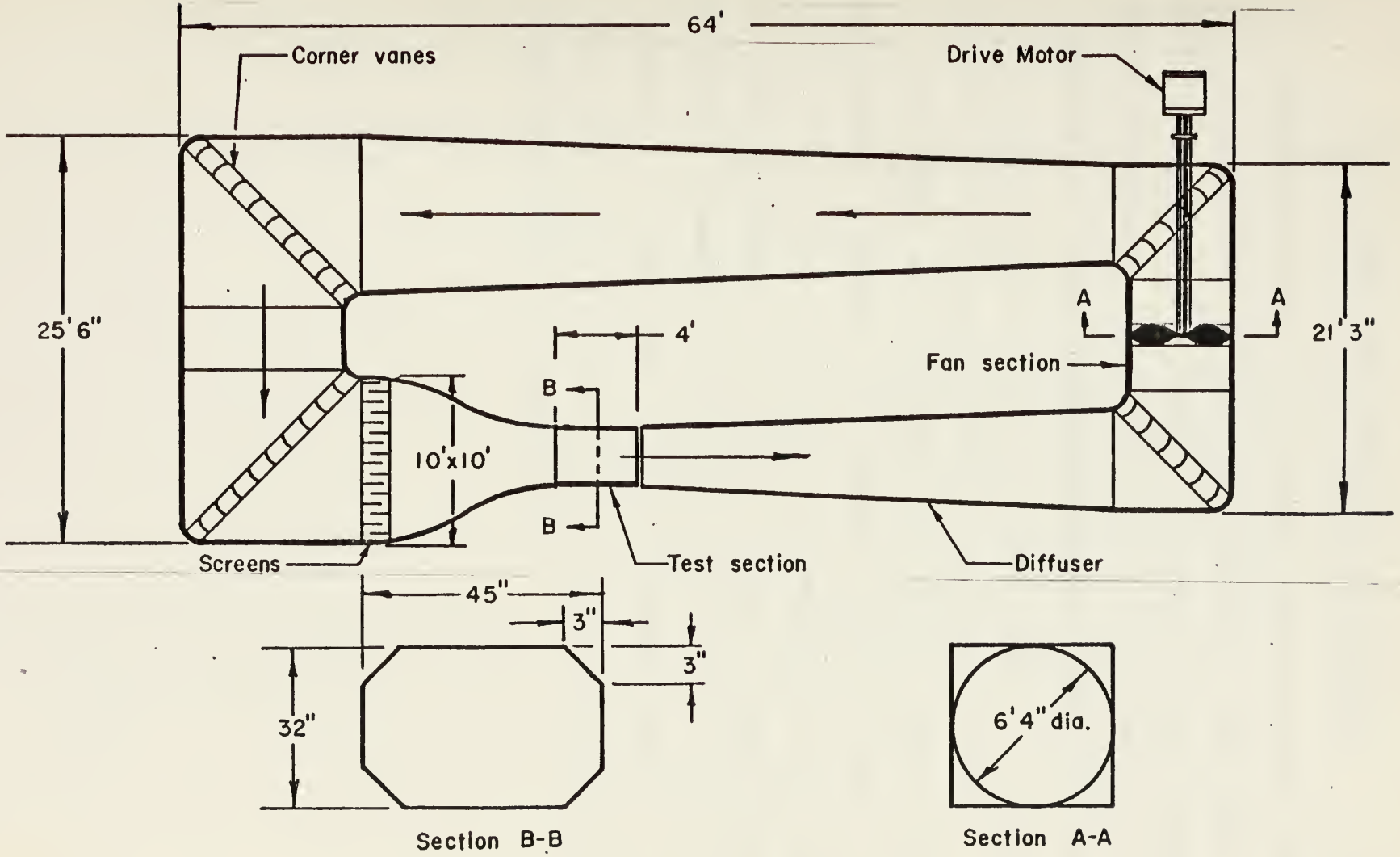

Figure 6

U. S. Naval Postgraduate School Low Speed Wind Tunnel

III. WIND TUNNEL EXTERNAL BEAM BALANCE

A three-component beam balance manufactured by Aerolab Development Company of Pasadena, California, was used to measure model aerodynamic drag forces. A drawing of this balance is shown in Figure 7. Lift force and pitching moment were of no consideration in this investigation due to the fact that it was the comparison of the drag force generated by the various models at several pitch angles that was of primary interest.

All models were mounted on two struts. The forward strut was rigidly attached to the balance central column and the aft strut to the pitch angle adjustment mechanism whose fulcrum was also attached to the central column. A forked bayonet mounting was used to attach the forward strut to the VGRB trunnions. The aft model trunnion attached directly to the pitch strut. The prolate spheroid model was attached to the respective struts at a single point.

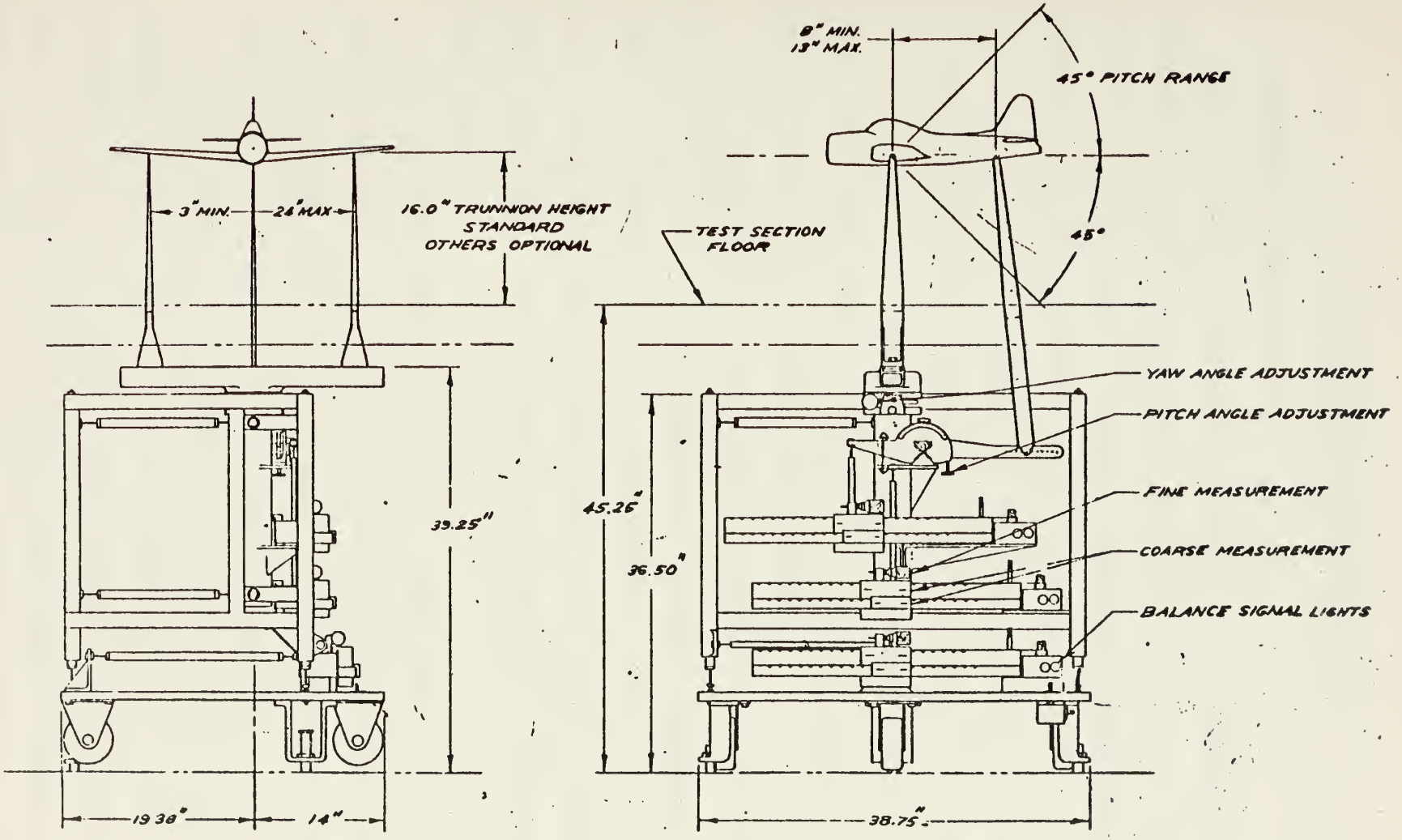

Figure 7

Aerolab Three-Component Beam Balance

IV. MODEL DESIGN AND DIMENSIONS

A. VARIABLE GEOMETRY RIGID BODIES

The choice of dimensions for the four rectangular plates comprising the parallelepiped center section of the VGRB was arbitrary. Each plate must have identical dimensions but the relationship between plate length and plate width is not critical. For the purposes of this investigation, the relationship between plate length and width was chosen such that the profile of the VGRB resembled that of an aircraft external fuel tank. Reference 1 provided insight into the drag characteristics of smooth geometric shapes.

The dimensions of the eight triangular plates forming each end section of the VGRB were, however, explicitly determined by the width of the parallelepiped rectangular plates and the somewhat arbitrarily chosen end section length. All VGRB dimensional relationships are derived in Appendix D of this report.

The overall dimensions of the VGRB models were,in part, determined by the size of the wind tunnel test section. It was determined that parallelepiped rectangular plate dimensions of three inch width by twelve inch length would meet the desired shape requirements and that different end section lengths would be used on the two VGRB models in order to investigate the effect of end length on the aerodynamic drag. The relationship between model and test section dimensions resulted in only a small blockage correction which was

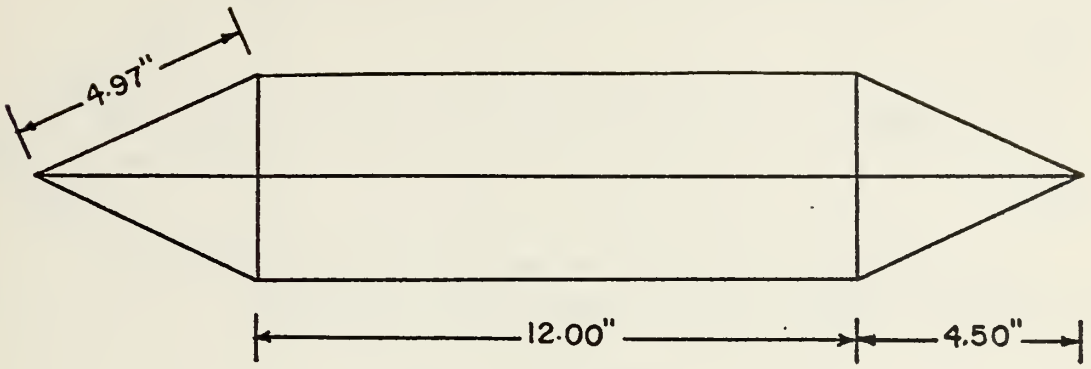

a. Top or Side View

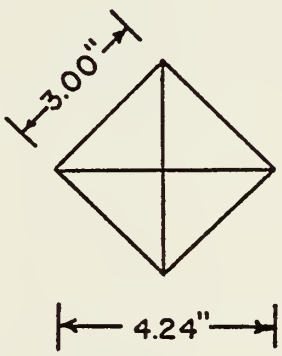

b. End View

Figure 8

Dimensions of Short, Full-Volume VGRB Model
(1/4 Scale)

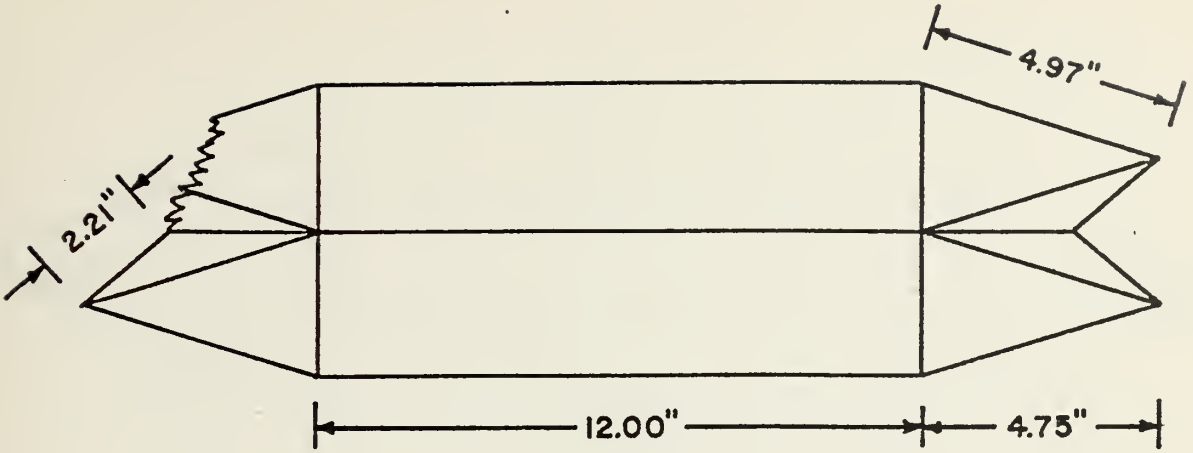

a. Top View

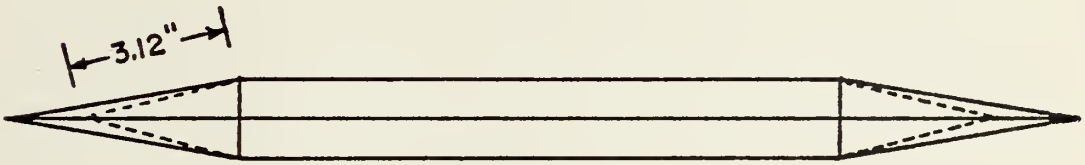

b. Side View

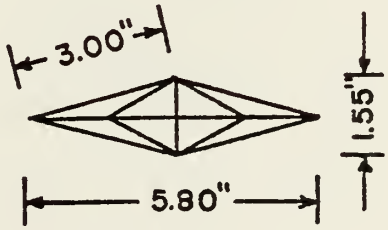

c. End View

Figure 9

Dimensions of Short, Half-Volume VGRB Model
(1/4 Scale)

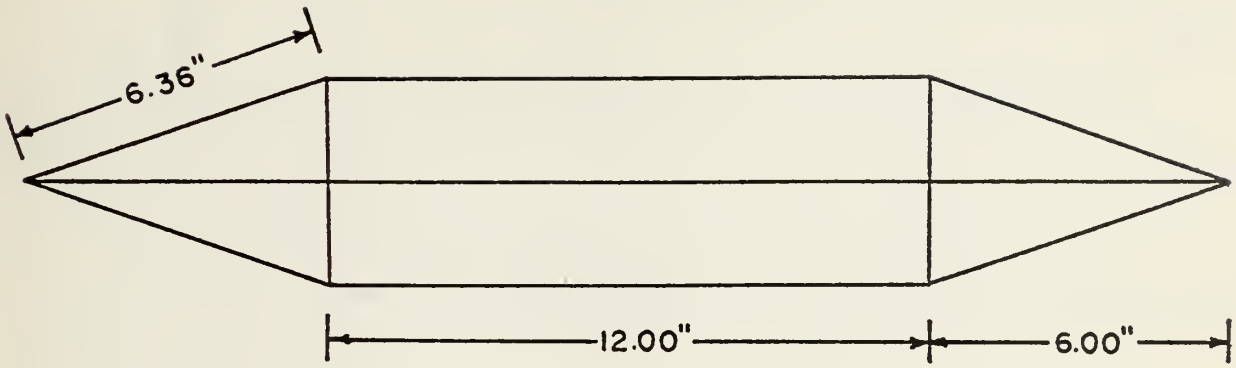

a. Top or Side View

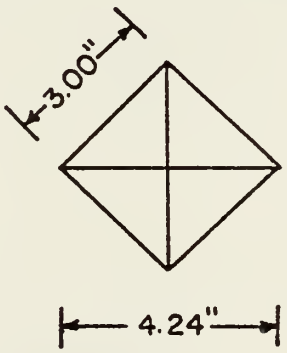

b. End View

Figure 10

Dimensions of Long, Full-Volume VGRB Model
(1/4 Scale)

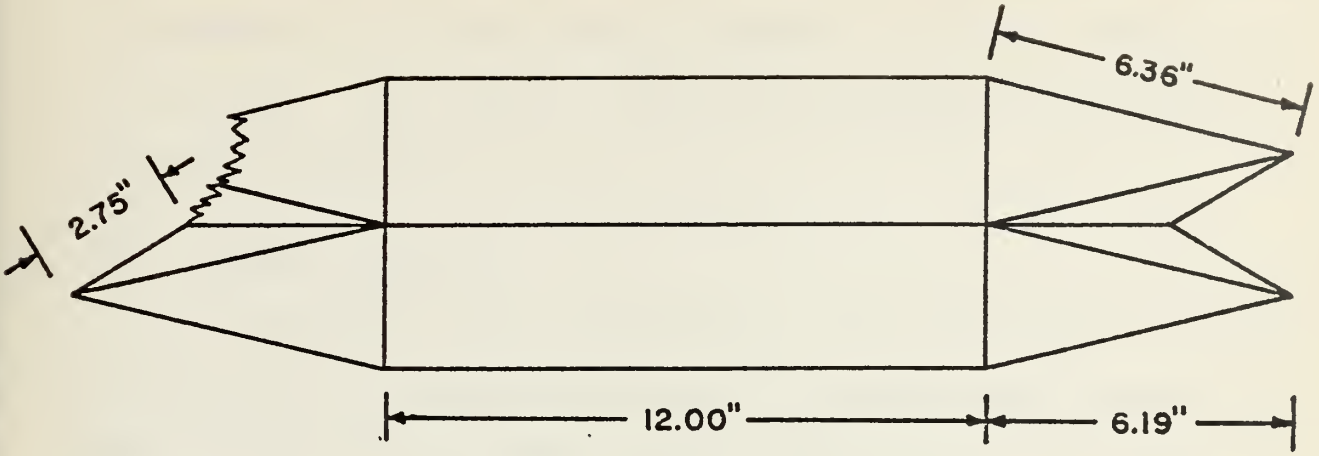

a. Top View

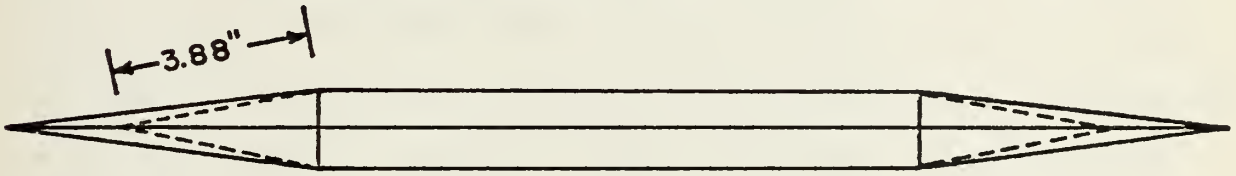

b. Side View

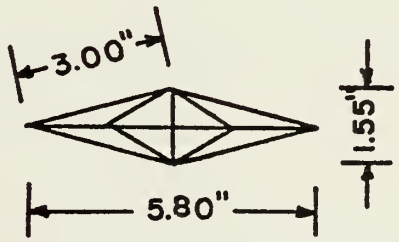

c. End View

Figure 11

Dimensions of Long, Half-Volume VGRB Model
(1/4 Scale)

accounted for in the coefficient of drag calculations contained in Appendix D of this report. Figures 8-11 detail VGRB model dimensions. For clarity, trunnion attachment point details have been omitted.

B. PROLATE SPHEROID

An elongated body of revolution was constructed in order to compare the aerodynamic drag of a smooth shape similar to that of an aircraft external fuel tank to that of a VGRB of identical length and volume. A prolate spheroid, generated by revolving an ellipse about its major axis, was constructed such that its volume and length were identical to those of the short, full-volume VGRB. Calculations required in determining the dimensions of this model are contained in Appendix D of this report. Figure 12 details prolate spheroid model dimensions.

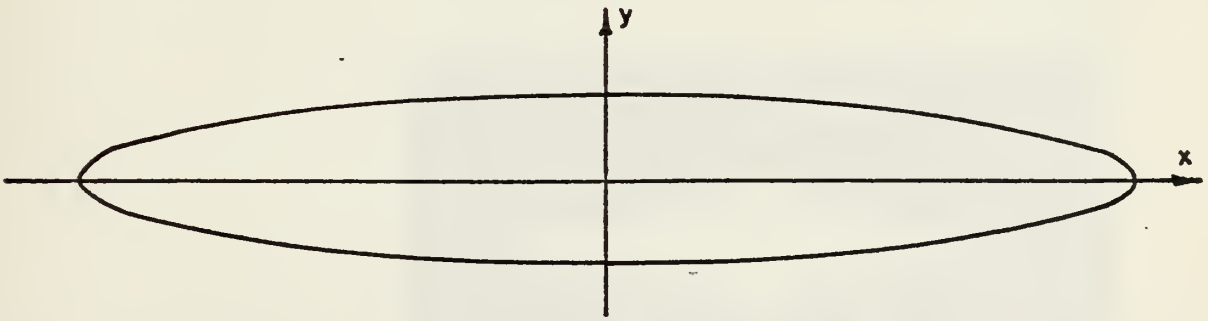

± x(inches)	± y(inches)	± x(inches)	± y(inches)
0	1.75	6	1.44
1	1.74	7	1.30
2	1.71	8	1.13
3	1.68	9	0.90
4	1.62	10	0.54
5	1.54	10.5	0

FIGURE 12. DIMENSIONS OF PROLATE SPHEROID MODEL

V. PROCEDURE

Aerodynamic drag forces were recorded for model pitch angles ranging from zero to sixteen degrees in two-degree increments as shown in Figures 13 and 14.

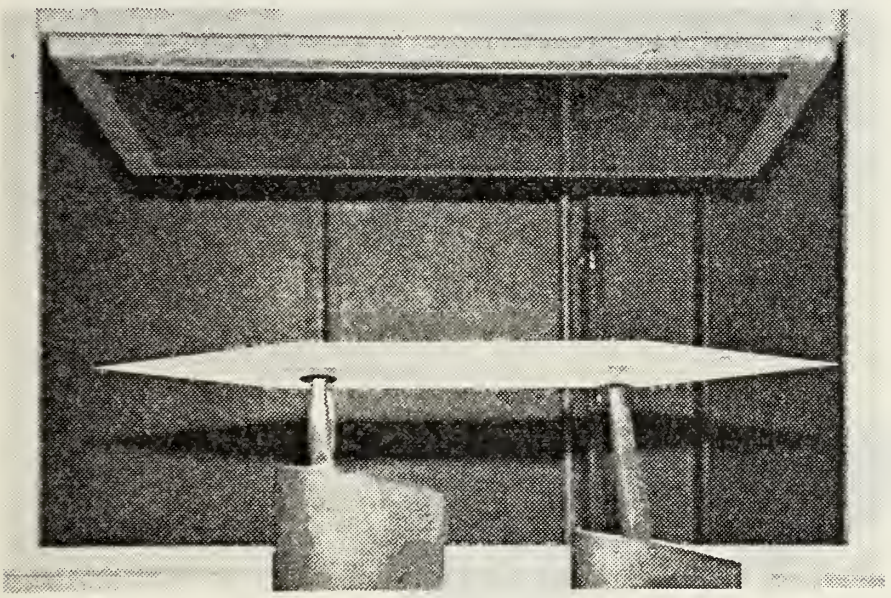

a. Side View

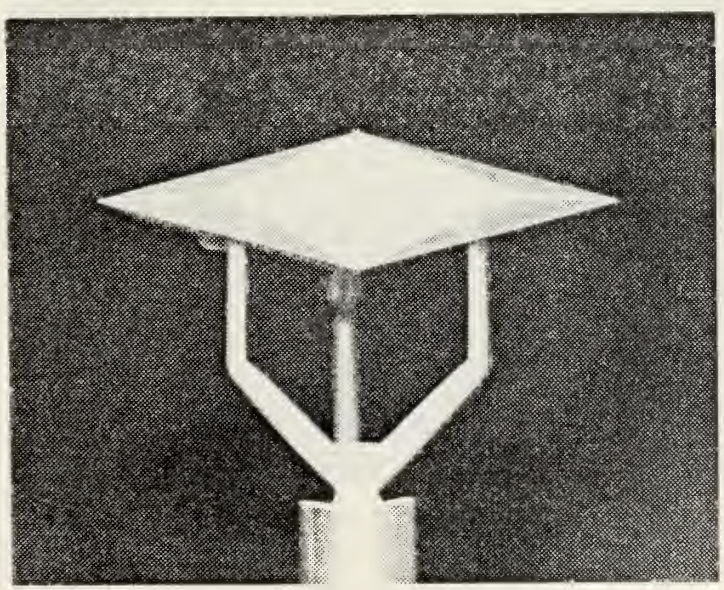

b. Front View

FIGURE 13. LONG, HALF-VOLUME VGRB AT ZERO DEGREES PITCH ANGLE

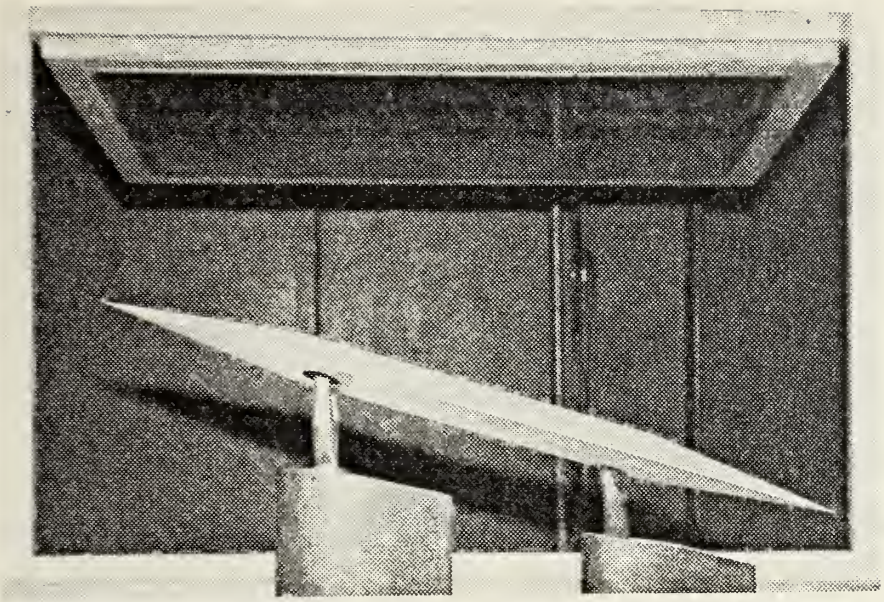

a. Side View

b. Front View

FIGURE 14. LONG, HALF-VOLUME VGRB AT SIXTEEN DEGREES PITCH ANGLE

Pitch-angle calibration was accomplished by positioning an inclinometer on the upper surface of the model, adjusting the balance pitch mechanism so that the inclinometer indicated the pitch angle desired, and recording the corresponding reading on the balance pitch-measurement quadrant. This procedure was followed for each model tested. In the case of the prolate spheroid, a pattern with a flat upper surface parallel to the model longitudinal axis was positioned so as to provide a flat surface for the inclinometer. Modeling clay was used to fair the model surface at the balance strut and bayonet attachment points.

In order to confirm consistency in the experimental results, all models were tested at two dynamic pressures: ten and forty-five centimeters of water, corresponding to approximately ninety and one-hundred-ninety miles per hour. At each pitch angle, tunnel speed was adjusted to maintain the appropriate dynamic pressure. In all cases, the model was cycled progressively from zero to sixteen degrees pitch angle. Gross drag was recorded to the nearest one-thousandth pound.

Support drag was measured by first removing the model and then fastening the forward bayonet and aft strut together with 0.032 inch stainless steel wire such that bayonet/strut separation was the same as that used when testing the model. Figure 14 shows the prolate spheroid supports in the wind tunnel test section prior to determining the support drag.

Support drag was recorded at both dynamic pressures and at the various pitch angles. To correct for the drag produced by that portion of the bayonet or strut that was imbedded in

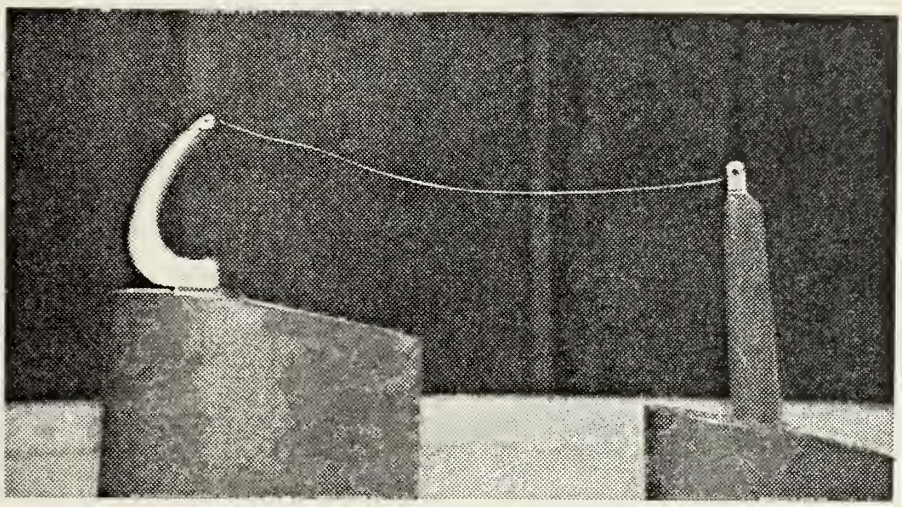

FIGURE 15. BAYONET AND STRUT CONFIGURATION FOR DETERMINING PROLATE SPHEROID SUPPORT DRAG

the model and for the drag introduced by the connecting wire, the support drag was reduced by ten percent in the case of the full-volume VGRB's and by five percent in the case of the half-volume VGRB's and the prolate spheroid. These corrections were based primarily on the magnitude of the reduction in support frontal area with the model installed. Net drag was obtained by subtracting the corrected support drag from the gross drag. A graphical presentation of net drag vs pitch angle is contained in Appendix B.

VI. DISCUSSION OF RESULTS

The results of this investigation are contained in tabular form in Appendix A, and graphically in Appendices B and C. Graphs were plotted using a Hewlett-Packard 9830A Calculator. The coefficients of a sixth-degree polynomial were determined using a least-squares curve fit and the results plotted by the auxiliary Plotter Pac. Each graph compares the drag force or the coefficient of drag of the full-volume VGRB with that of the corresponding half-volume VGRB at a specific tunnel dynamic pressure. Also included are graphs of the drag force and coefficient of drag of the prolate spheroid as compared with those of the short VGRB.

The experimental results obtained at a tunnel dynamic pressure of ten centimeters of water are consistent with those recorded at forty-five centimeters of water. In every case, the drag of the half-volume VGRB at small pitch angles was less than that of the corresponding full-volume VGRB. This was to be expected as the frontal area of the half-volume VGRB was half that of the full volume VGRB at zero degrees pitch angle. As pitch angle was increased, however, the drag of the half-volume VGRB approached that of the full-volume configuration and beyond approximately five degrees pitch angle, the aerodynamic drag of the half-volume VGRB exceeded that of the corresponding full-volume model. At the maximum pitch angle of sixteen degrees, the drag of the half-volume VGRB was more than double that of the corresponding full-volume model. The

large difference resulted primarily from the increase in the projected frontal area due to the flattening of the VGRB as its volume was reduced.

In both the full-volume and half-volume configurations, the aerodynamic drag of the short and long Variable Geometry Rigid Bodies at small pitch angles was nearly identical. Above four degrees pitch angle the drag of the long VGRB was found to be greater than that of the short one due, once again, to the greater projected frontal area.

Of considerable interest was the comparison of the aerodynamic drag of the prolate spheroid to that of the VGRB. At each pitch angle tested, the drag of the prolate spheroid was less than that of the short, equal-volume VGRB in both configurations. Throughout the range of pitch angles investigated, the prolate spheroid drag increased by approximately 100 percent as compared with 270 percent for the full-volume VGRB and 850 percent for the half-volume VGRB.

VII. CONCLUSIONS

This investigation indicates that the aerodynamic drag of a VGRB in either the full-volume or half-volume configuration is greater than that of a similar prolate spheroid. This was found to be true at all pitch angles investigated. The use of a collapsible structure designed and oriented as were the VGRB's in this experiment appears to offer no aerodynamic benefit as compared to a similar, less complex, ellipsoid.

There are several considerations affecting the results which were not accounted for in the course of this investigation and which may have a significant effect on VGRB aerodynamic drag.

The half-volume VGRB most likely generates considerable lift, resulting in induced drag, at positive angles of attack. It is believed that the induced drag will increase as the VGRB transitions from the full-volume to the zero-volume configuration. An investigation of the aerodynamic lift generated by a VGRB at positive pitch angles would provide data from which the magnitude of the induced drag could be determined.

The interference drag, a result of the strut/model interface, has not been accounted for due to the complexity of the required support equipment. It is possible that this component of drag would be of the same order of magnitude as the strut form drag, especially in the presence of the previously

mentioned lift. Consideration of this induced interference drag may result in a net drag less than that which was obtained in this investigation.

The VGRB models tested were oriented in the wind tunnel test section so that they collapsed in the horizontal plane. An increase in pitch angle thus presented a corresponding increase in the flat-plate area presented to the air flow. By rotating the models ninety degrees about their longitudinal axis, they would collapse in the vertical plane resulting in entirely different drag characteristics as pitch angle is changed. An investigation of such an orientation would provide an interesting comparison with the prolate spheroid, especially at large pitch angles.

APPENDIX A: TABLES

TABLE 1

SHORT VGRB DRAG DATA
DYNAMIC PRESSURE = 10 cm H_2O

Pitch Angle (degrees)	Gross Drag (pounds)	Support Drag (pounds)	Corrected Support Drag (pounds)	Model Drag (pounds)	Calculated Coefficient of Drag ($x10^3$)
			FULL VOLUME		
0	0.374	0.136	0.124	0.250	1.352
2	0.384	0.134	0.122	0.262	1.417
4	0.398	0.132	0.120	0.278	1.503
6	0.428	0.132	0.120	0.308	1.666
8	0.470	0.131	0.119	0.351	1.898
10	0.542	0.130	0.118	0.424	2.293
12	0.656	0.128	0.116	0.540	2.920
14	0.803	0.124	0.113	0.690	3.731
16	0.966	0.122	0.111	0.855	4.624
			HALF VOLUME		
0	0.363	0.179	0.170	0.193	1.043
2	0.371	0.178	0.169	0.202	1.092
4	0.409	0.176	0.167	0.242	1.308
6	0.491	0.174	0.165	0.326	1.763
8	0.617	0.172	0.163	0.454	2.455
10	0.821	0.169	0.161	0.660	3.569
12	1.114	0.166	0.158	0.956	5.170
14	1.461	0.163	0.155	1.306	7.062
16	1.907	0.159	0.151	1.756	9.496

TABLE 2

SHORT VGRB DRAG DATA
DYNAMIC PRESSURE = 45 cm H_2O

Pitch Angle (degrees)	Gross Drag (pounds)	Support Drag (pounds)	Corrected Support Drag (pounds)	Model Drag (pounds)	Calculated Coefficient of Drag ($x10^3$)
			FULL VOLUME		
0	1.454	0.584	0.531	0.923	1.109
2	1.517	0.582	0.529	0.988	1.187
4	1.579	0.578	0.525	1.054	1.267
6	1.701	0.575	0.523	1.178	1.416
8	1.920	0.571	0.519	1.401	1.684
10	2.208	0.567	0.515	1.693	2.034
12	2.701	0.562	0.511	2.190	2.632
14	3.392	0.558	0.507	2.885	3.467
16	4.161	0.554	0.504	2.657	4.395
			HALF VOLUME		
0	1.426	0.688	0.654	0.772	0.927
2	1.458	0.671	0.637	0.821	0.986
4	1.617	0.653	0.620	0.997	1.198
6	2.015	0.642	0.610	1.405	1.688
8	2.618	0.631	0.599	2.019	2.426
10	3.548	0.626	0.595	2.953	3.548
12	4.806	0.621	0.590	4.216	5.066
14	6.311	0.617	0.586	5.725	6.879
16	8.321	0.613	0.582	7.739	9.300

TABLE 3

LONG VGRB DRAG DATA
DYNAMIC PRESSURE = 10 cm H_2O

Pitch Angle (degrees)	Gross Drag (pounds)	Support Drag (pounds)	Corrected Support Drag (pounds)	Model Drag (pounds)	Calculated Coefficient of Drag ($x10^3$)
			FULL VOLUME		
0	0.373	0.136	0.124	0.249	1.346
2	0.377	0.134	0.122	0.255	1.379
4	0.397	0.132	0.120	0.277	1.498
6	0.426	0.132	0.120	0.306	1.655
8	0.483	0.131	0.119	0.364	1.968
10	0.554	0.130	0.118	0.436	2.358
12	0.676	0.128	0.116	0.560	3.028
14	0.827	0.124	0.113	0.714	3.861
16	1.012	0.122	0.111	0.901	4.873
			HALF VOLUME		
0	0.367	0.179	0.170	0.197	1.065
2	0.380	0.178	0.169	0.211	1.141
4	0.417	0.176	0.167	0.250	1.352
6	0.513	0.174	0.165	0.348	1.778
8	0.568	0.172	0.163	0.405	2.550
10	0.857	0.169	0.161	0.696	3.764
12	1.194	0.166	0.158	1.036	5.602
14	1.519	0.163	0.155	1.364	7.376
16	2.031	0.159	0.151	1.880	10.167

TABLE 4

LONG VGRB DRAG DATA
DYNAMIC PRESSURE = 45 cm H_2O

Pitch Angle (degrees)	Gross Drag (pounds)	Support Drag (pounds)	Corrected Support Drag (pounds)	Model Drag (pounds)	Calculated Coefficient of Drag ($x10^3$)
			FULL VOLUME		
0	1.370	0.584	0.531	0.839	1.008
2	1.390	0.582	0.529	0.861	1.035
4	1.474	0.578	0.525	0.949	1.140
6	1.651	0.575	0.523	1.128	1.355
8	1.884	0.571	0.519	1.365	1.640
10	2.219	0.567	0.515	1.704	2.048
12	2.746	0.562	0.511	2.235	2.686
14	3.526	0.558	0.507	3.019	3.628
16	4.304	0.554	0.504	3.800	4.566
			HALF VOLUME		
0	1.438	0.688	0.654	0.784	0.942
2	1.477	0.671	0.637	0.840	1.009
4	1.644	0.653	0.620	1.024	1.230
6	2.077	0.642	0.610	1.467	1.763
8	2.792	0.631	0.599	2.193	2.635
10	3.689	0.626	0.595	3.094	3.718
12	5.225	0.621	0.590	4.635	5.570
14	6.702	0.617	0.586	6.116	7.349
16	8.904	0.613	0.582	8.322	10.001

TABLE 5

PROLATE SPHEROID DRAG DATA

Pitch Angle (degrees)	Gross Drag (pounds)	Support Drag (pounds)	Corrected Support Drag (pounds)	Model Drag (pounds)	Calculated Coefficient of Drag ($\times 10^3$)
		DYNAMIC PRESSURE = 10 cm H_2O			
0	0.240	0.102	0.097	0.143	0.773
2	0.240	0.099	0.094	0.146	0.789
4	0.245	0.097	0.092	0.153	0.827
6	0.252	0.097	0.092	0.160	0.865
8	0.264	0.097	0.092	0.172	0.929
10	0.282	0.097	0.092	0.190	1.027
12	0.305	0.097	0.092	0.213	1.152
14	0.336	0.092	0.087	0.249	1.346
16	0.379	0.087	0.083	0.296	1.600
		DYNAMIC PRESSURE = 45 cm H_2O			
0	1.108	0.485	0.461	0.647	0.777
2	1.112	0.480	0.456	0.656	0.788
4	1.121	0.470	0.447	0.674	0.809
6	1.136	0.464	0.441	0.695	0.835
8	1.216	0.457	0.434	0.782	0.939
10	1.292	0.463	0.440	0.852	1.024
12	1.400	0.468	0.445	0.955	1.147
14	1.539	0.462	0.439	1.100	1.322
16	1.740	0.459	0.436	1.304	1.567

APPENDIX B: Net Drag vs Pitch Angle

Figure 16
Short VGRB
Net Drag
vs
Pitch Angle

(Dynamic pressure = 10 cm H_2O)

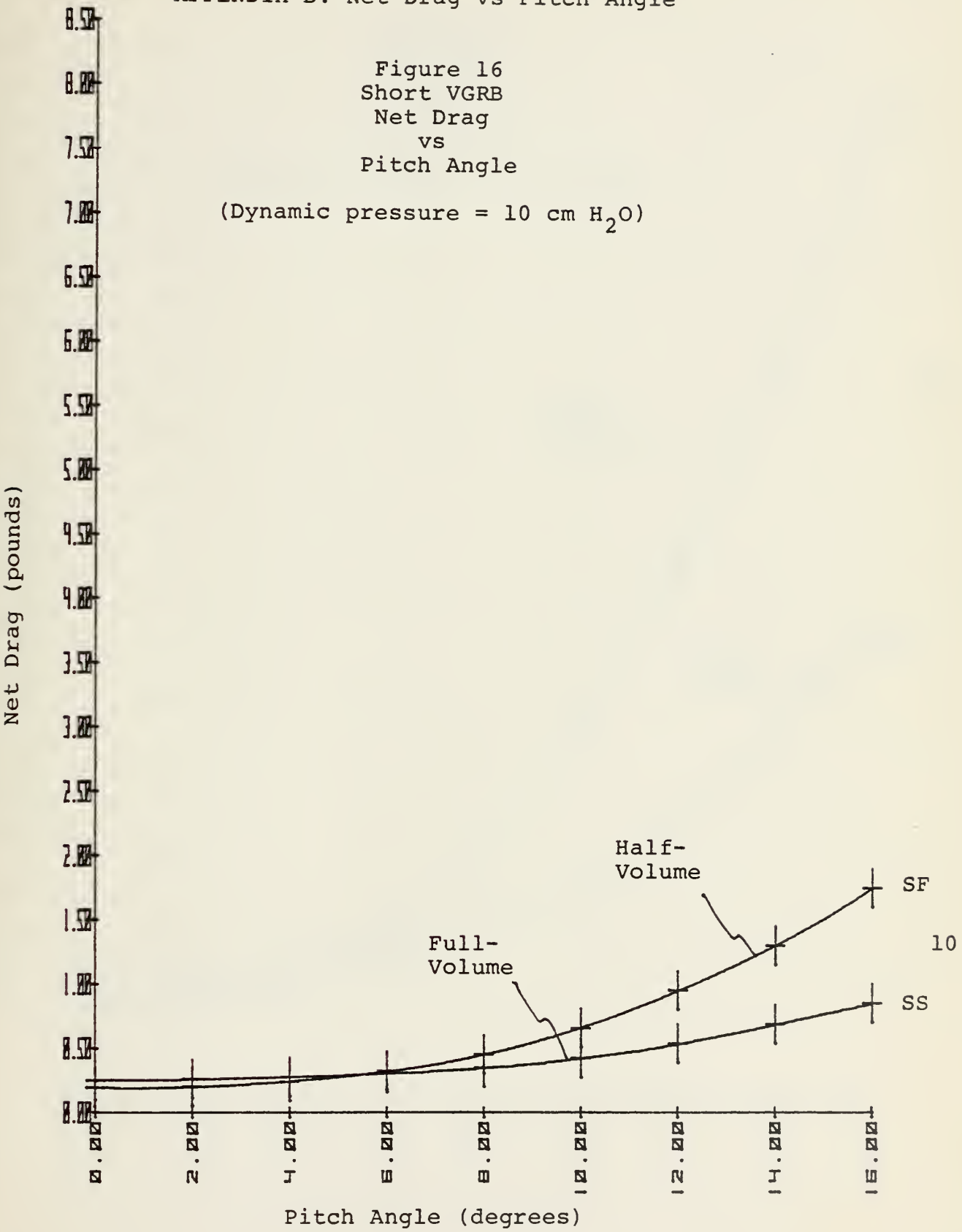

Figure 17
Short VGRB
Net Drag
vs
Pitch Angle

(Dynamic pressure = 45 cm H_2O)

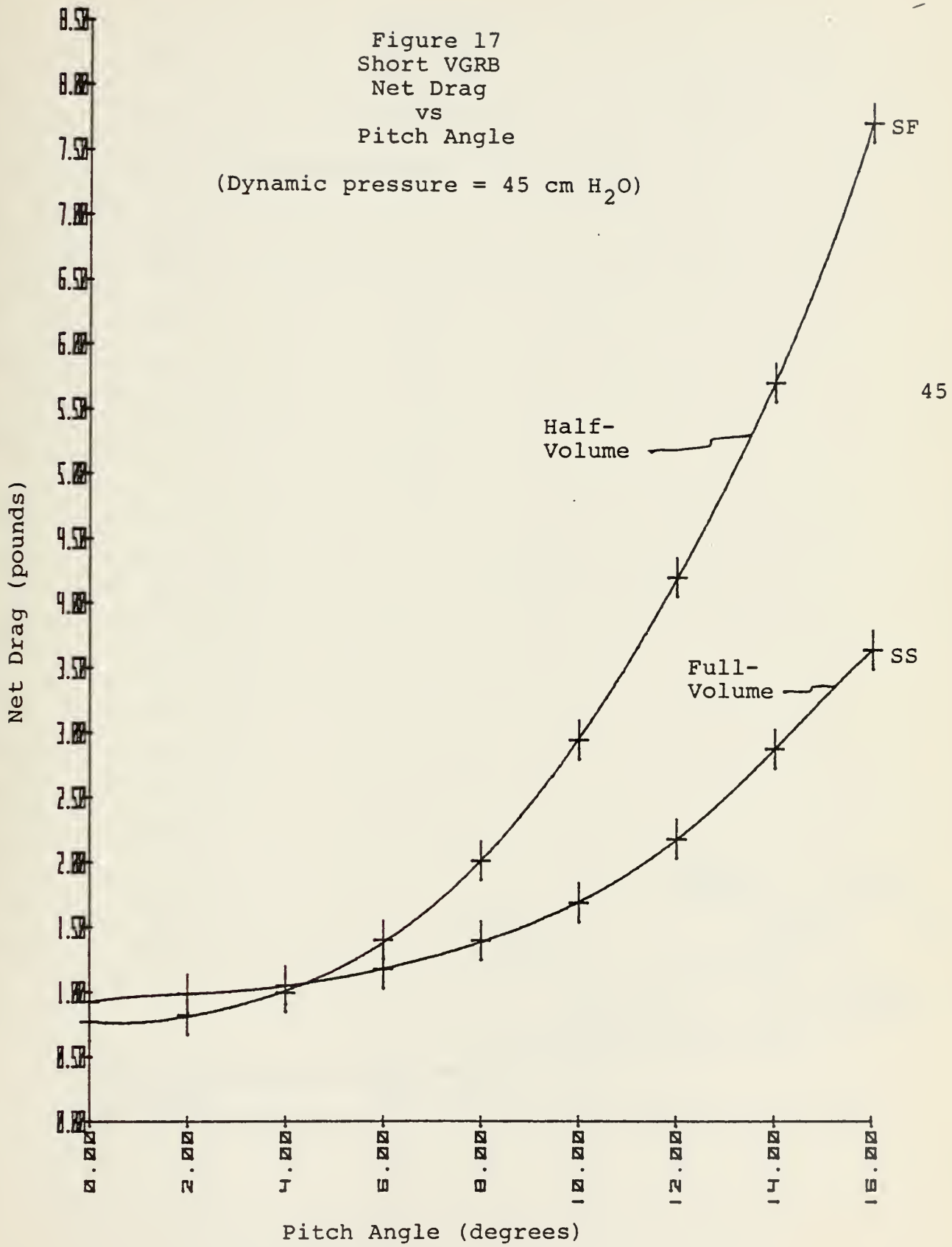

Figure 18
Long VGRB
Net Drag
vs
Pitch Angle

(Dynamic pressure = 10 cm H_2O)

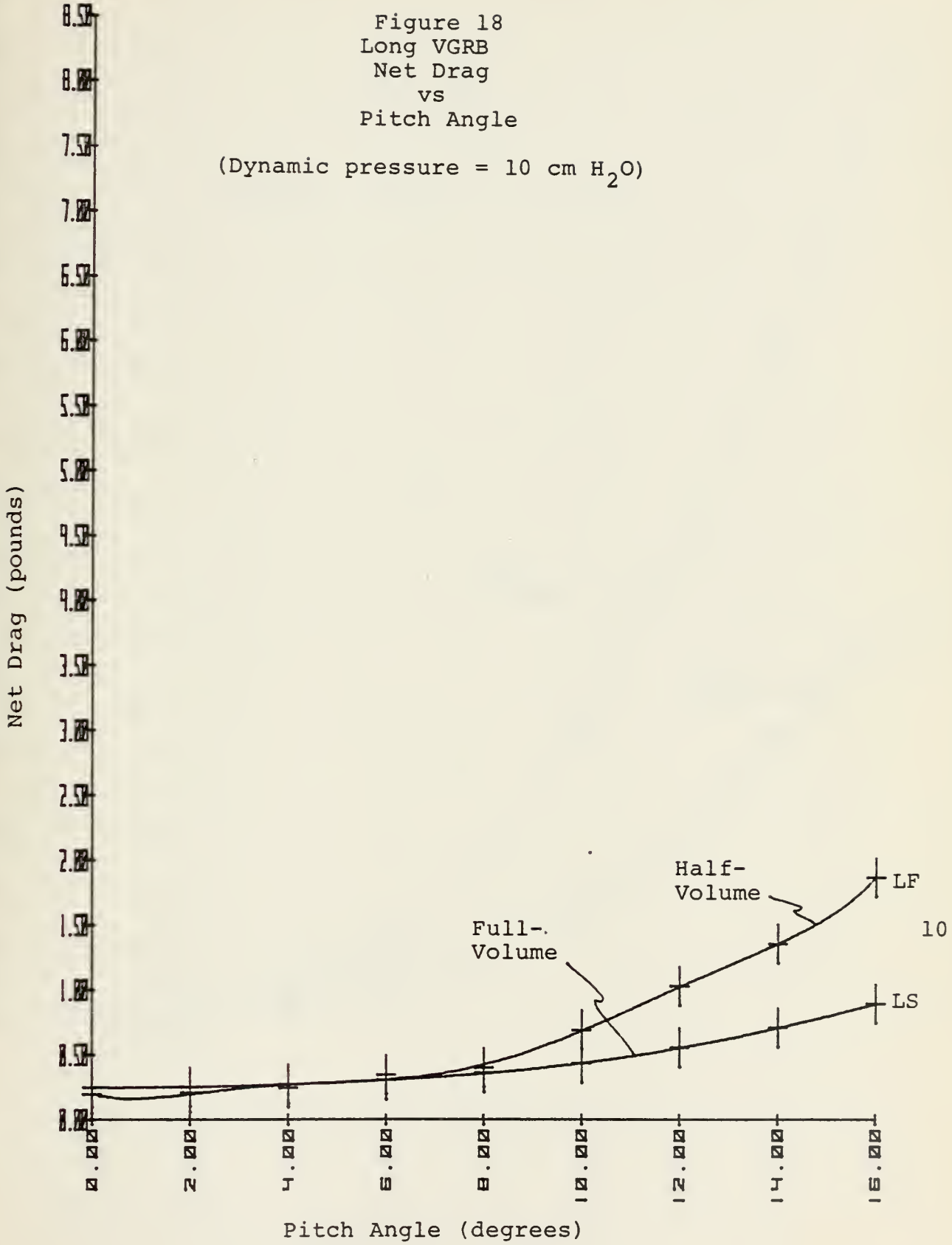

Figure 19
Long VGRB
Net Drag
vs
Pitch Angle

(Dynamic pressure = 45 cm H_2O)

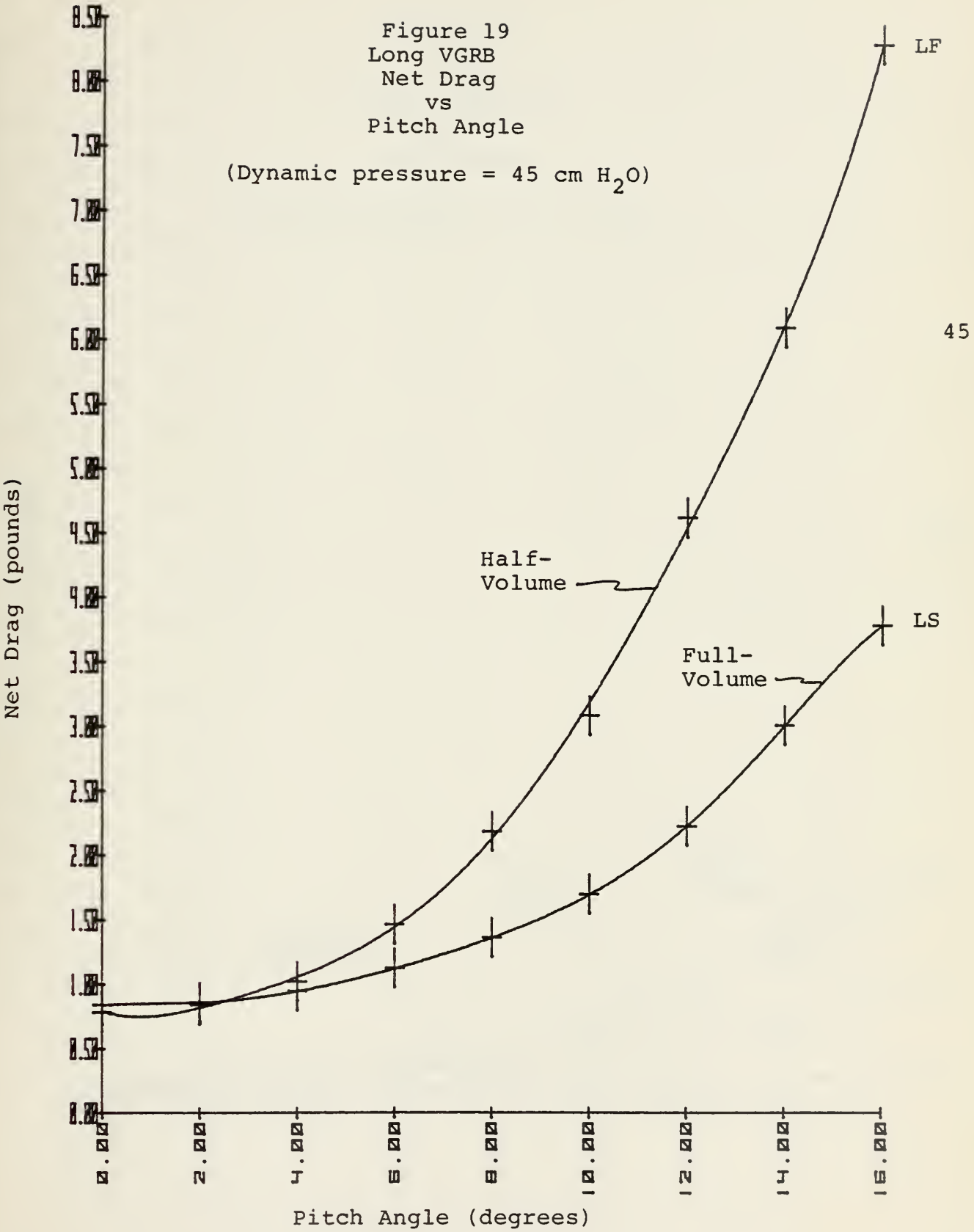

Figure 20
Short VGRB
and
Prolate Spheroid
Net Drag
vs
Pitch Angle

(Dynamic pressure = 10 cm H_2O)

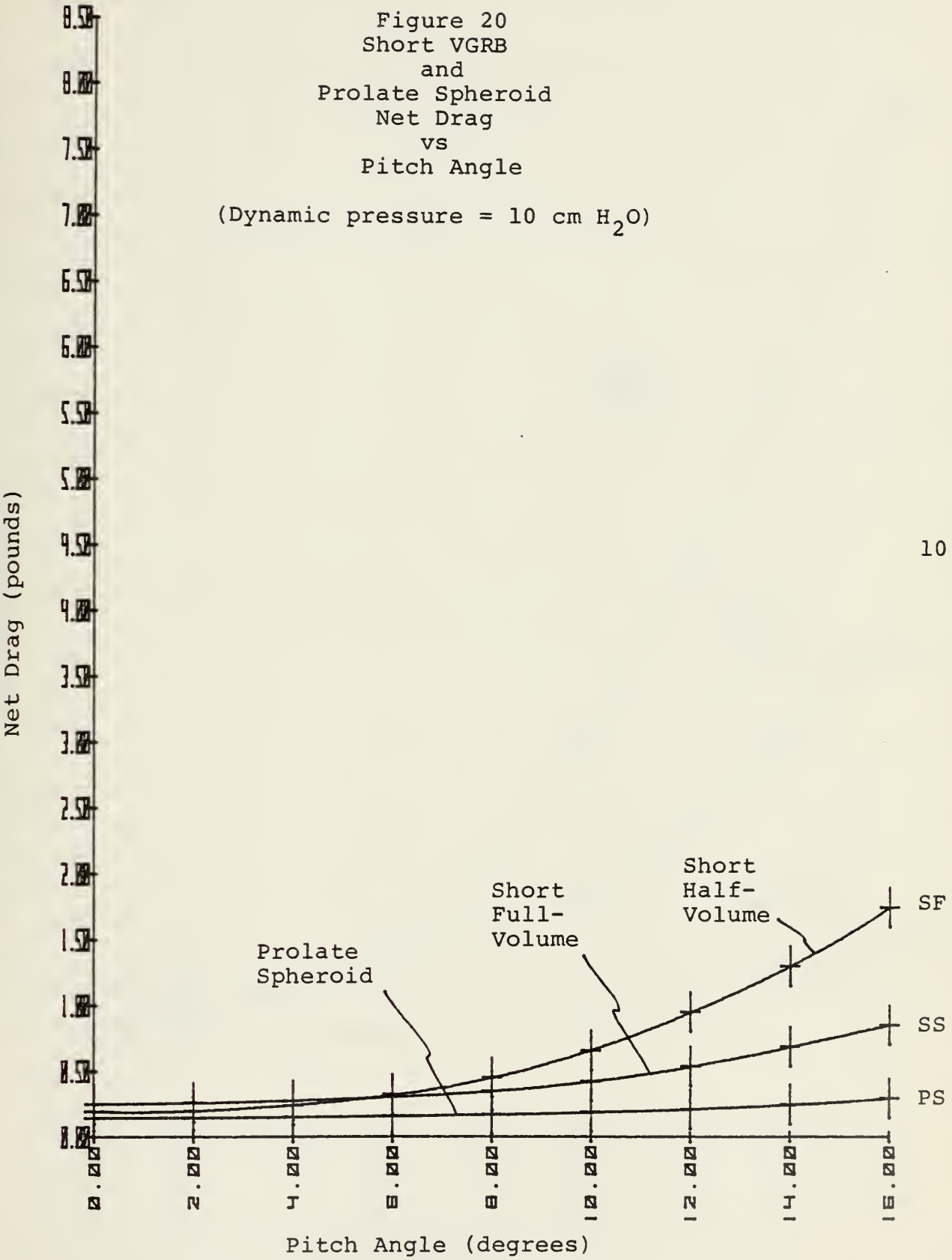

Figure 21
Short VGRB
and
Prolate Spheroid
Net Drag
vs
Pitch Angle

(Dynamic pressure = 45 cm H_2O)

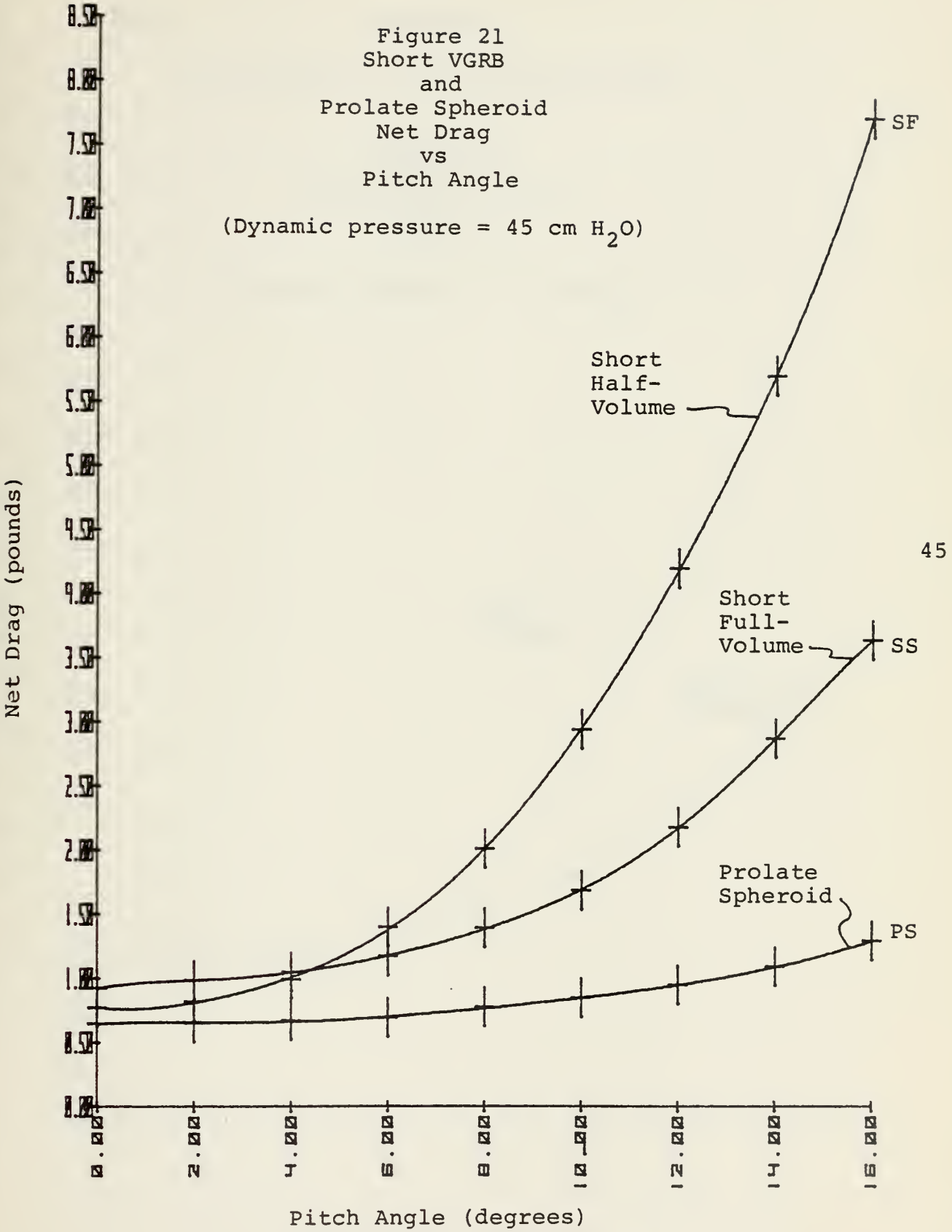

APPENDIX C

Coefficient of Drag vs Pitch Angle

Figure 22
Short VGRB
Coefficient of Drag
vs
Pitch Angle

(Dynamic pressure = 10 cm H_2O)

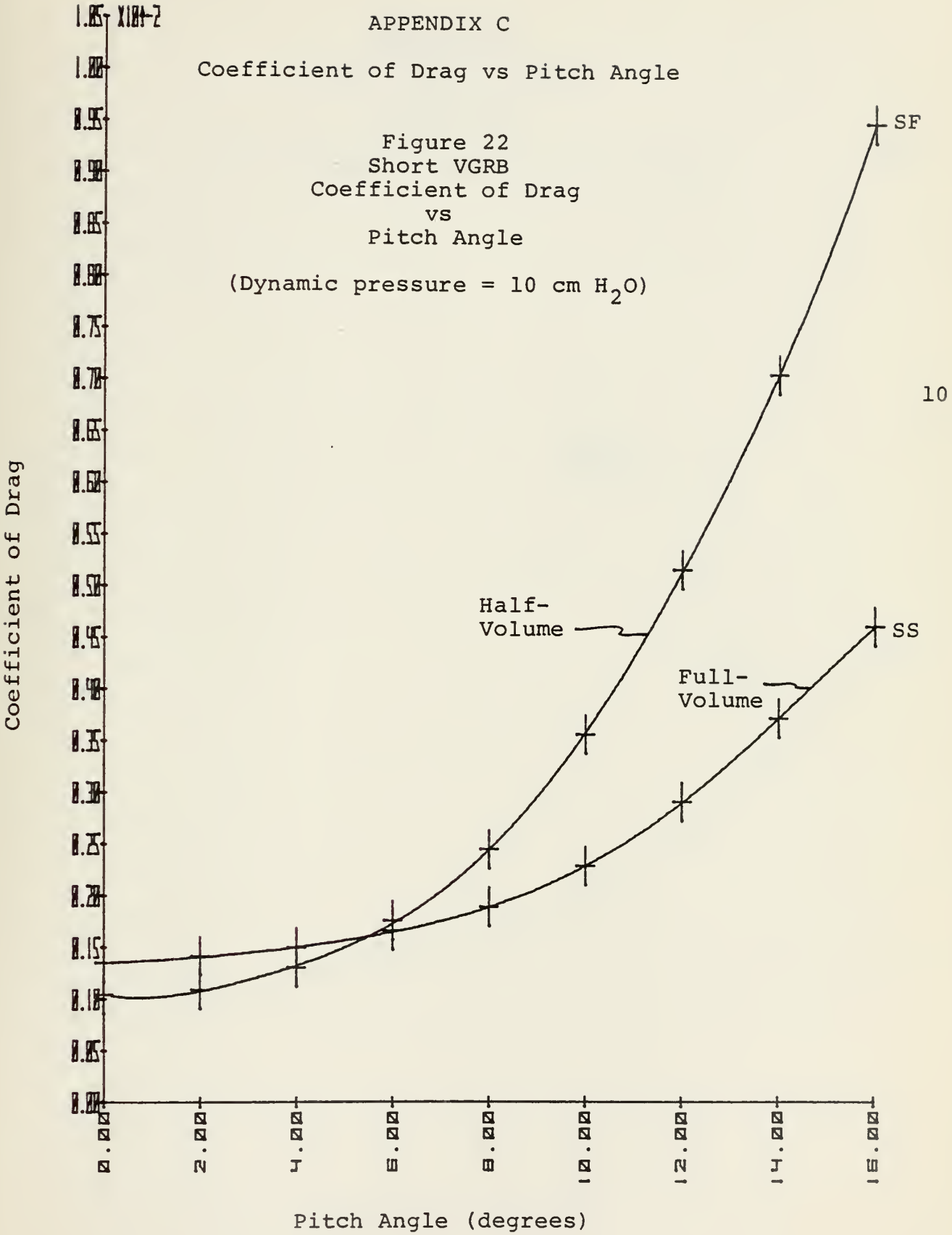

Figure 23
Short VGRB
Coefficient of Drag
vs
Pitch Angle

(Dynamic pressure = 45 cm H_2O)

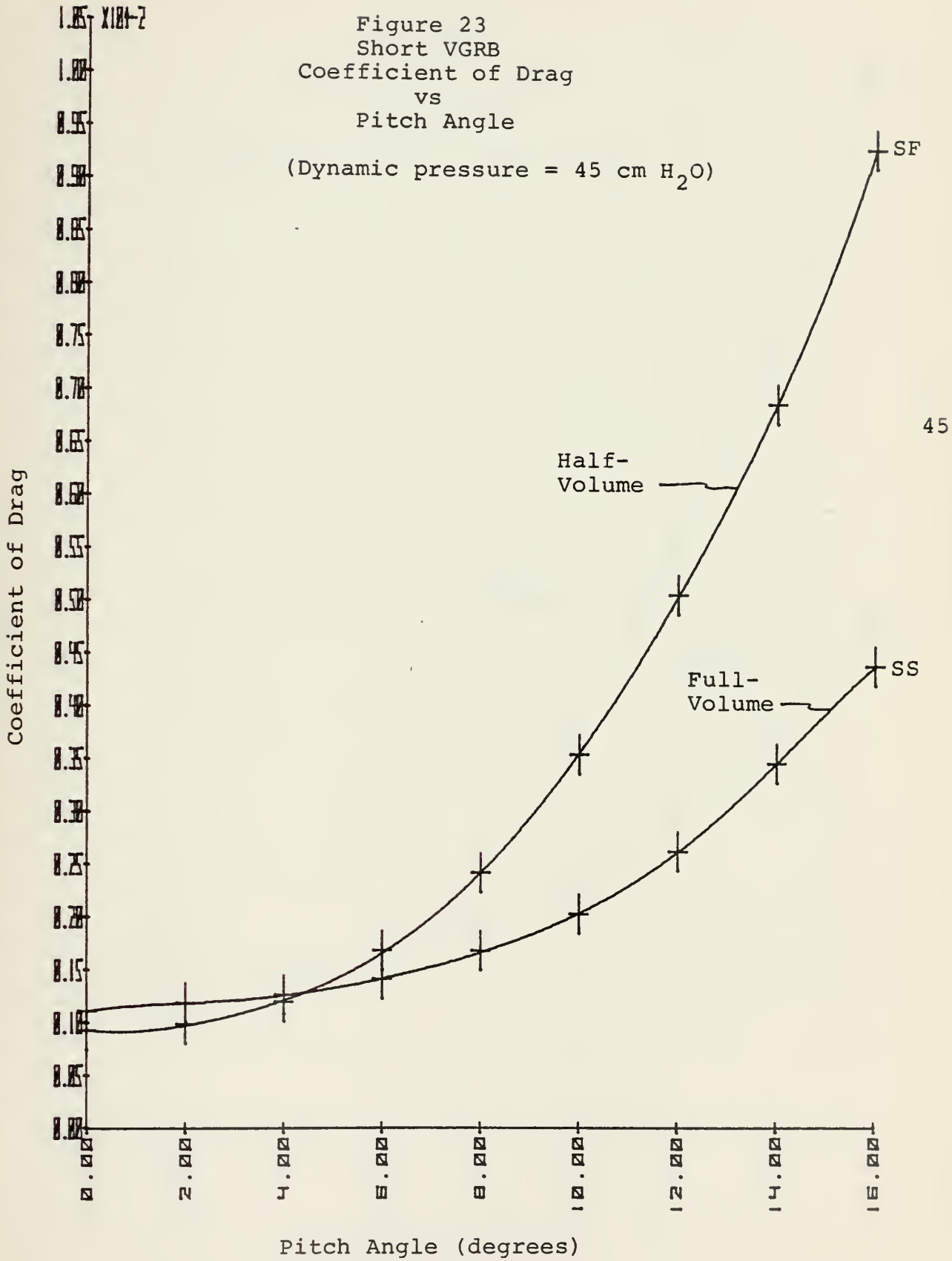

Figure 24
Long VGRB
Coefficient of Drag
vs
Pitch Angle

(Dynamic pressure = 10 cm H_2O)

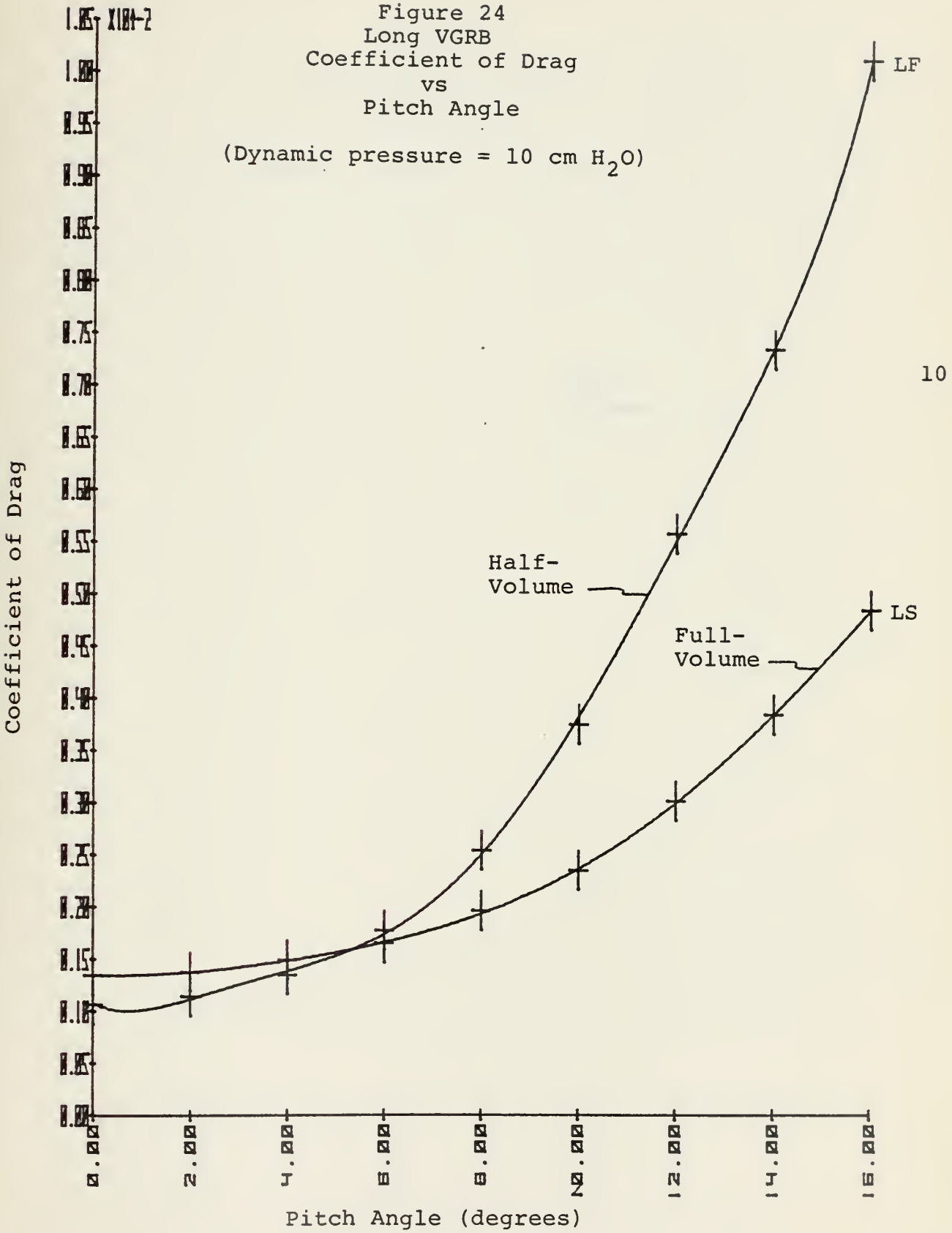

Figure 25
Long VGRB
Coefficient of Drag
vs
Pitch Angle

(Dynamic pressure = 45 cm H_2O)

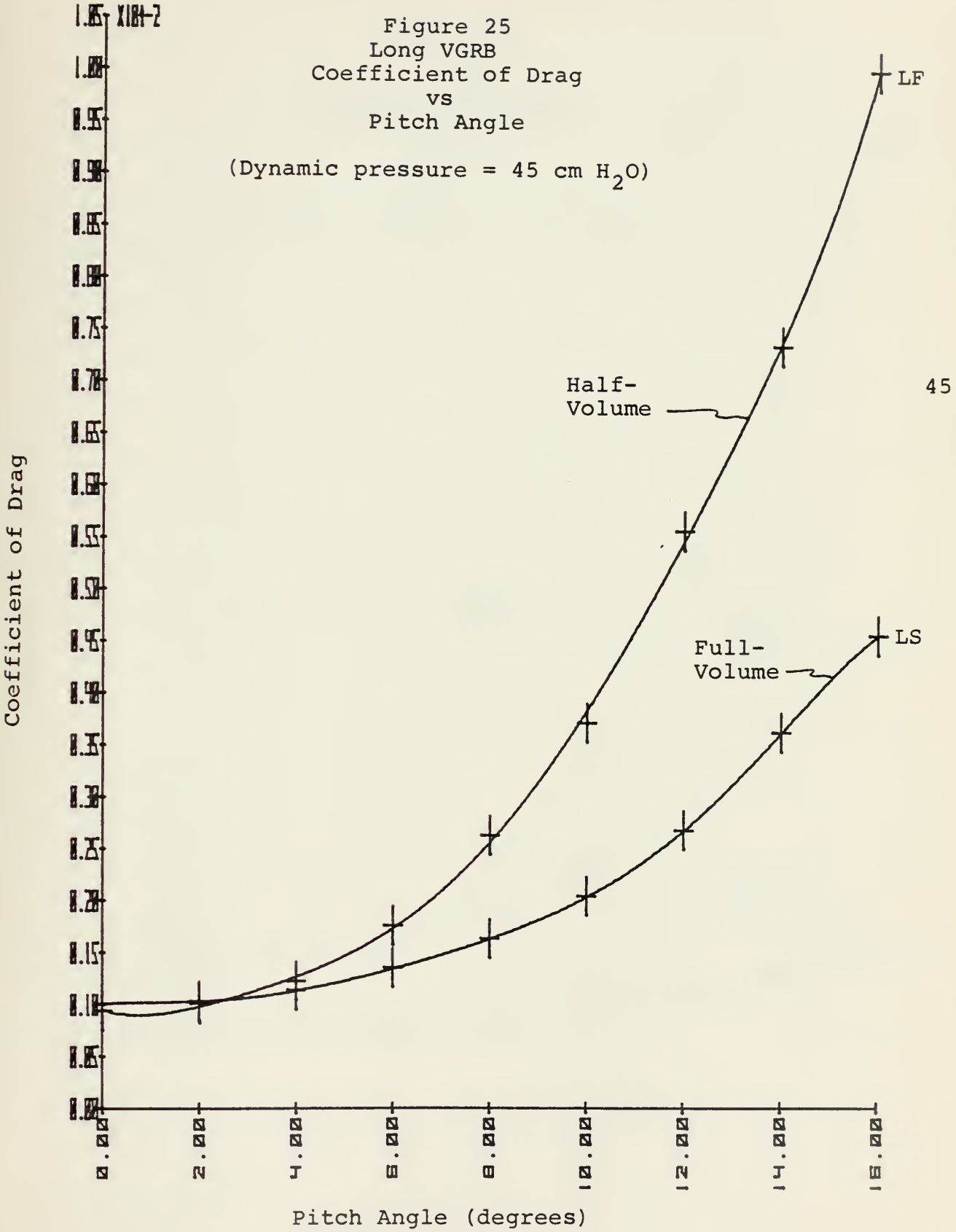

Figure 26
Short VGRB
and
Prolate Spheroid
Coefficient of Drag
vs
Pitch Angle

(Dynamic pressure = 10 cm H_2O)

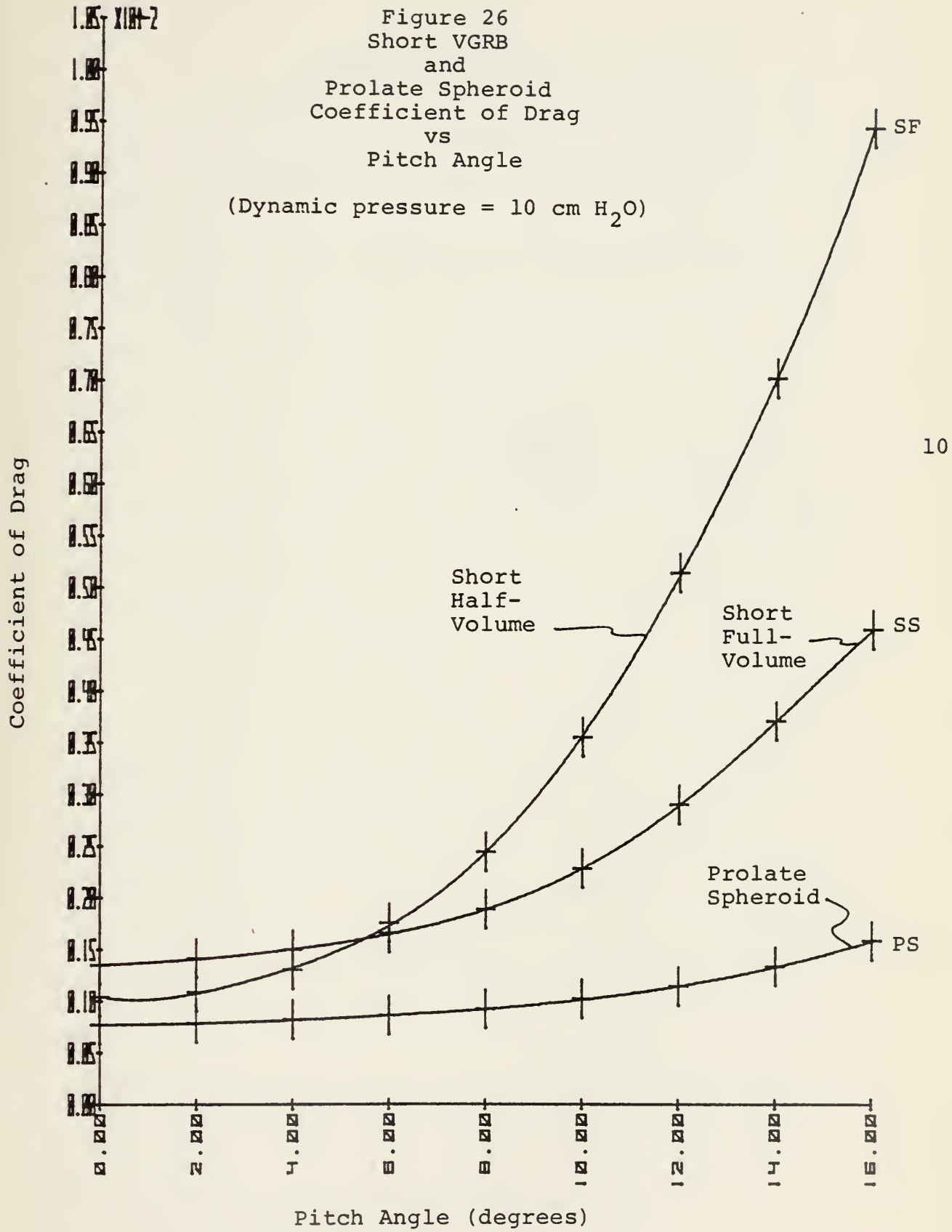

Figure 27
Short VGRB
Prolate Spheroid
Coefficient of Drag
vs
Pitch Angle

(Dynamic pressure = 45 cm H_2O)

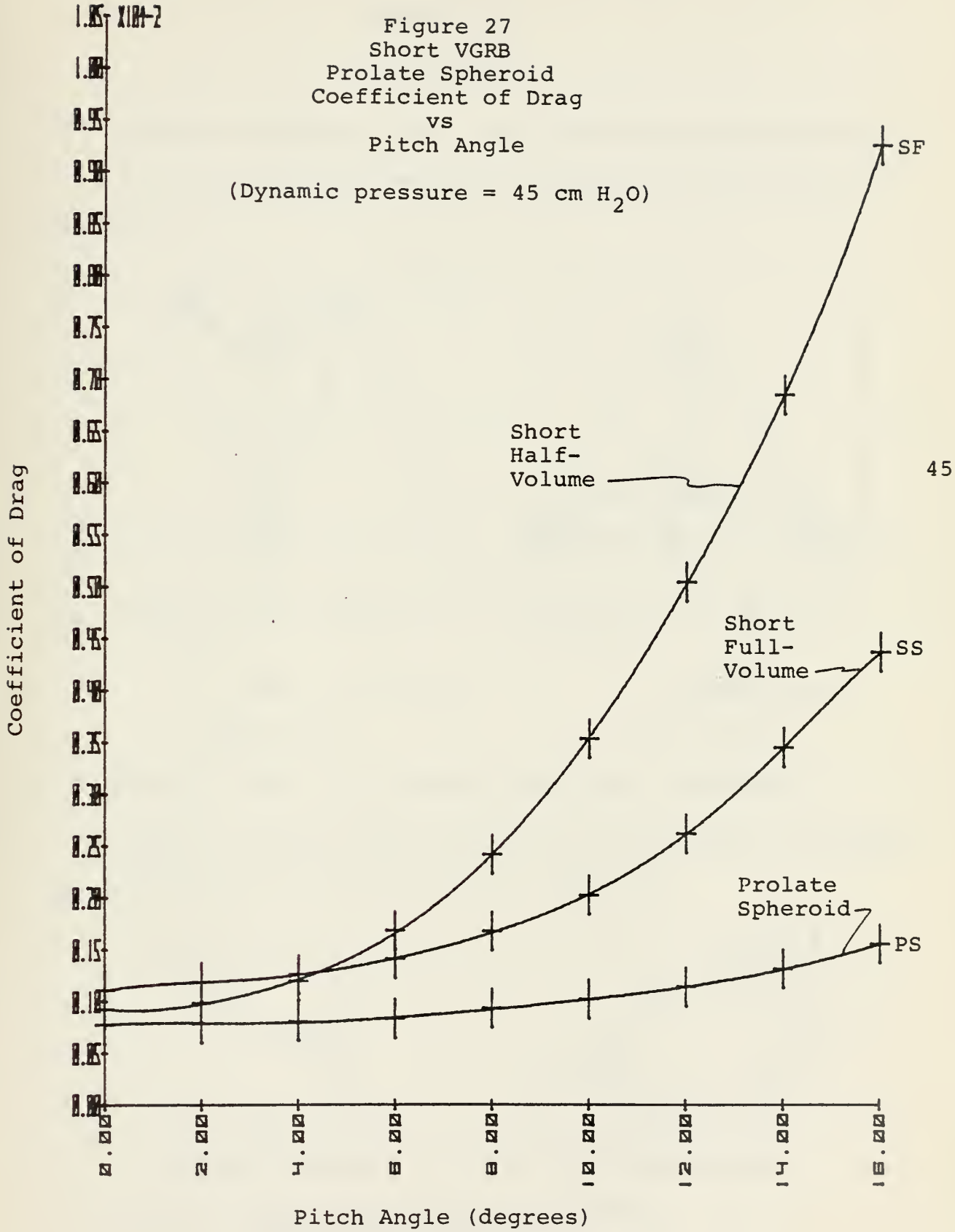

APPENDIX D

CALCULATIONS

A. VARIABLE GEOMETRY RIGID BODY DIMENSIONAL RELATIONSHIPS

VGRB end section dimensional parameters are defined in Figure 28.

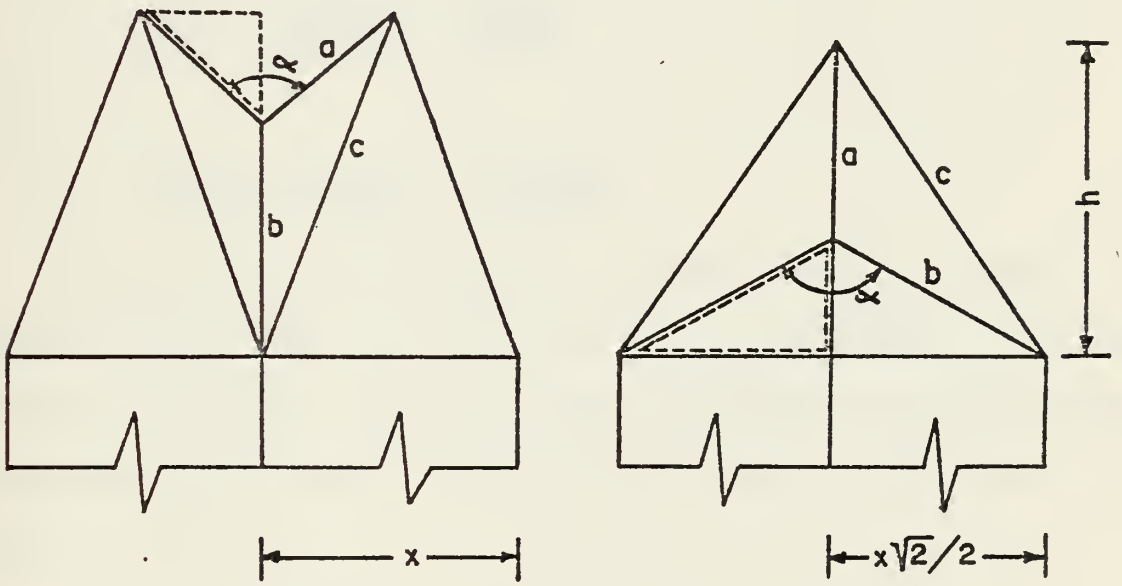

a. Zero-Volume b. Full-Volume

FIGURE 28. VGRB END SECTION DIMENSIONAL PARAMETERS

Figure 29 depicts the dimensional relationship triangles represented by the dotted lines in Figure 28.

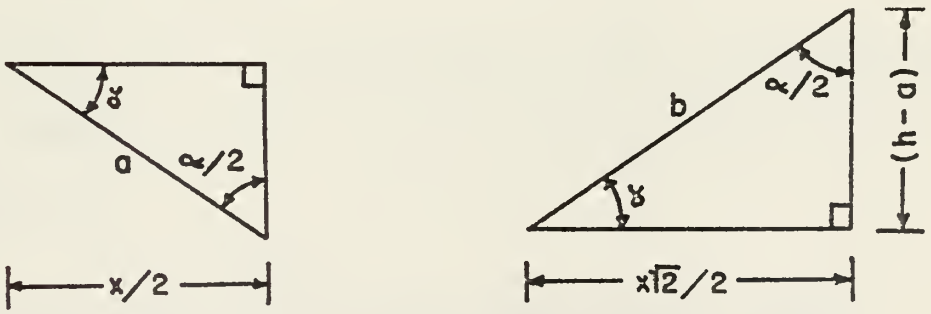

a. Zero-Volume b. Full-Volume

FIGURE 29. VGRB END SECTION DIMENSIONAL RELATIONSHIP TRIANGLES

The dimensional relationship triangles shown in Figure 29 are geometrically similar from which it is evident that

$$a\sqrt{2} = b \tag{1}$$

The remaining parameters shown in Figure 29 are related such that

$$\text{Cos}\,\gamma = \frac{x\sqrt{2}/2}{a\sqrt{2}} = x/2a$$

$$\text{Tan}\,\gamma = \frac{(h-a)}{x\sqrt{2}/2} = \frac{2(h-a)}{x\sqrt{2}}$$

and

$$\text{Tan}\left[\text{Cos}^{-1}\left(\frac{x}{2a}\right)\right] = \frac{2(h-a)}{x\sqrt{2}} \tag{2}$$

With the aid of collapsible cardboard models it was determined that there is a lower limit on the length of the end section that will allow structural integrity to be maintained throughout the range of VGRB configurations. This limit dictates that

$$h \geq 1.5x$$

must be maintained.

To investigate the drag characteristic of a minimum length VGRB, the short model was designed such that

$$h = 1.5x.$$

Due primarily to consideration of the wind tunnel test section dimensions and to the VGRB profile desired, it was determined that

$$x = 3 \text{ inches}$$

for both the short and the long VGRB models tested.

An iterative solution of equation (2) yields, for the short VGRB,

$$a = 2.208 \text{ inches.}$$

It follows directly from equation (1) that

$$b = 3.123 \text{ inches.}$$

The relative complexity of the end section folding triangles is directly related to end section length. It was decided that little was to be gained by testing a VGRB with extremely long end sections although such a design was physically possible. The end section for the long VGRB model was designed such that

$$h = 2x.$$

Following the same procedure as outlined above for the short VGRB model, it was determined that for the long model,

$$a = 2.745 \text{ inches}$$

and

$$b = 3.882 \text{ inches.}$$

B. DIMENSIONAL RELATIONSHIPS BETWEEN A FULL-VOLUME AND HALF-VOLUME VARIABLE GEOMETRY RIGID BODY

The volume of a VGRB is directly related to the cross-sectional area of the parallelepiped center section. In order to construct a model of a half-volume VGRB, it was necessary to determine the dimensions of a rhombic cross section whose area was equal to half that of a corresponding full-volume cross section. Figure 30 depicts the parameters used in deriving the half-volume VGRB cross sectional dimensional relationships.

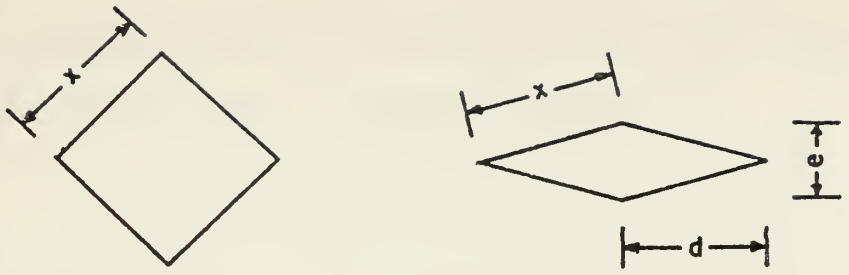

a. Full-Volume b. Half-Volume

FIGURE 30. VGRB CROSS SECTIONAL DIMENSIONAL PARAMETERS

The cross sectional area of the full-volume VGRB center section is simply

$$A_f = x^2.$$

The cross sectional area of the corresponding half-volume center section is, by definition,

$$A_h = A_h/2.$$

From basic geometry it follows that

$$A_h = x^2/2 = 2\ (\tfrac{1}{2}\ ed) \tag{3}$$

and

$$d = \left[x^2 - (\tfrac{e}{2})^2\right]^{1/2}. \tag{4}$$

Substituting equation (4) into equation (3) and simplifying yields

$$x^4 - 4e^2x^2 + e^4 = 0. \tag{5}$$

Substituting the previously determined x dimension of three inches into equation (5) and solving for e by iteration yields

$$e = 1.553 \text{ inches}.$$

C. PROLATE SPHEROID DIMENSIONAL RELATIONSHIP

A prolate spheroid is generated by revolving an ellipse about its major axis, as shown in Figure 31.

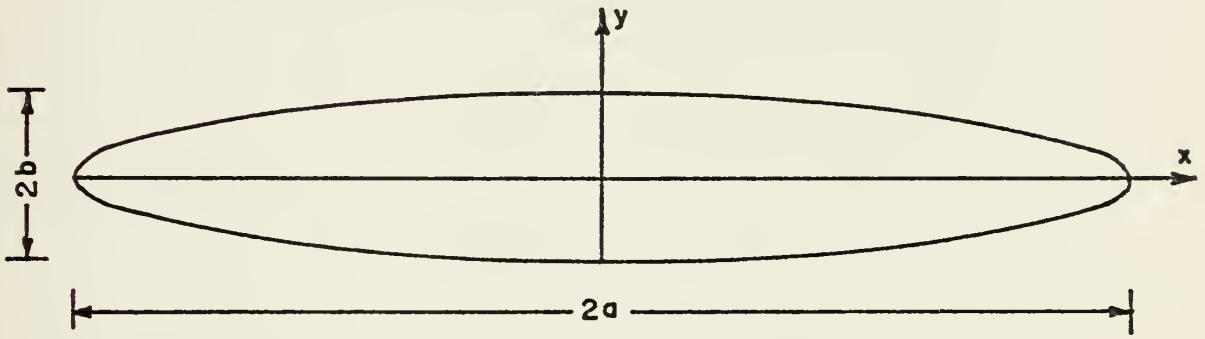

FIGURE 31. PROLATE SPHEROID (1/4 SCALE)

The prolate spheroid model constructed for this investigation was designed such that its length and volume were equal to the length and volume of the short, full-volume VGRB model shown in Figure 32.

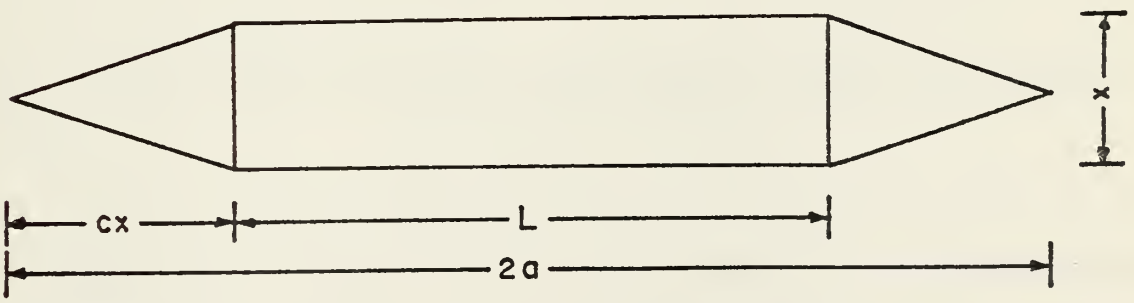

FIGURE 32. SHORT, FULL-VOLUME VGRB (1/4 SCALE)

From Figure 32 it follows that the volume of the short, full-volume VGRB is

$$V = x^2 L + 2\left[\frac{1}{3} x^2 (ax)\right]$$

or

$$V = x^2 L + 2/3\ ax^3$$

and

$$a = cx + L/2.$$

Given that

$$x = 3 \text{ inches},$$

$$L = 12 \text{ inches}$$

and

$$C = 1.5,$$

then for the short, full-volume VGRB model

$$V = 135 \text{ cubic inches}$$

and

$$a = 10.5 \text{ inches}.$$

The volume of a prolate spheroid is given by

$$V = 4/3\ \pi ab^2$$

which, after substituting the known model volume and length, yields

$$b = 1.752 \text{ inches}.$$

Referring to Figure 31, the equation of an ellipse defining the prolate spheroid model longitudinal cross section,

$$\frac{x^2}{a^2} + \frac{y^2}{b^2} = 1,$$

can now be solved for y given that x varies from -a to +a. The resulting values of x and y are shown in Figure 12.

D. COEFFICIENT OF DRAG

The coefficient of drag, Cd, is defined to be

$$Cd = \frac{D}{qS}$$

where

D = drag force,

q = corrected dynamic pressure,

and

S = characteristic model area.

The drag force, in pounds, was determined directly using the wind tunnel balance.

The corrected dynamic pressure is related to the uncorrected dynamic pressure, q_u, such that

$$q = q_u(1+2E)$$

where E is the total blockage factor. Reference 2 states that if doubt exists as to the applicability of aerodynamic blockage equations to unusual shapes, or in cases where large wakes exist due to separated flow, the total blockage factor may be determined by

$$E = 1/4 \frac{\text{model frontal area}}{\text{test section area.}}$$

Model frontal area at zero degrees pitch angle and test section area are known. The corrected dynamic pressure can easily be determined after converting the uncorrected dynamic pressure from centimeters of water to pounds per square foot.

Reference 2 also states that for non-lifting bodies where only drag coefficients are involved, the projected frontal area of the model is used as the characteristic area. It was

determined that the projected frontal area of the full-volume VGRB at zero degrees pitch angle would provide the most satisfactory characteristic area. This is simply the cross sectional area of the VGRB center section in the full-volume configuration. This value for S, namely 9 in^2, has been used in all drag coefficient calculations, including those for the prolate spheroid.

The results of the coefficient of drag calculations are contained in Appendix C.

LIST OF REFERENCES

1. Fluid-Dynamic Drag, Sighard F. Hoerner, 1965.

2. Laboratory Manual for Low Speed Wind-Tunnel Testing, Department of Aeronautics, Naval Postgraduate School.

INITIAL DISTRIBUTION LIST

		No. Copies
1.	Defense Documentation Center Cameron Station Alexandria, Virginia 22314	2
2.	Library, Code 0212 Naval Postgraduate School Monterey, California 93940	2
3.	Department Chairman, Code 67 Department of Aeronautics Naval Postgraduate School Monterey, California 93940	1
4.	Associate Professor D. M. Layton, Code 67Ln Department of Aeronautics Naval Postgraduate School Monterey, California 93940	1
5.	LCDR Larry D. Pfitzenmaier 308 Dorothy Avenue Ventura, California 93003	1